A Spatial-Random-Process Based Multidisciplinary System Uncertainty Propagation Approach with Model Uncertainty

Zhen Jiang
Department of Mechanical Engineering, Northwestern University
Evanston, IL 60208
e-mail: zhenjiang2015@u.northwestern.edu

Wei Li
School of Aeronautics, Northwestern Polytechnical University
Xi'an, Shaanxi 710072, P. R. China
e-mail: liwiair@gmail.com

Daniel W. Apley
Department of Industrial Engineering & Management Sciences, Northwestern University
Evanston, IL 60208
e-mail: dapley@northwestern.edu

Wei Chen[1]
Department of Mechanical Engineering, Northwestern University
Evanston, IL 60208
e-mail: weichen@northwestern.edu

ABSTRACT

The performance of a multidisciplinary system is inevitably affected by various sources of uncertainties, usually categorized as aleatory (e.g. input variability) or epistemic (e.g. model uncertainty) uncertainty. In the framework of design under uncertainty, all sources of uncertainties should be aggregated to assess the uncertainty of system quantities of interest (QOIs). In a multidisciplinary design system, uncertainty propagation refers to the analysis that quantifies the overall uncertainty of system QOIs resulting from all sources of aleatory and epistemic uncertainty originating in the individual disciplines. However, due to the complexity of multidisciplinary simulation, especially the coupling relationships between individual disciplines, many uncertainty propagation approaches in

[1] Corresponding author.

the existing literature only consider aleatory uncertainty and ignore the impact of epistemic uncertainty. In this paper, we address the issue of efficient uncertainty quantification of system QOIs considering both aleatory and epistemic uncertainties. We propose a spatial-random-process (SRP) based multidisciplinary uncertainty analysis (MUA) method that, subsequent to SRP-based disciplinary model uncertainty quantification, fully utilizes the structure of SRP emulators and leads to compact analytical formulas for assessing statistical moments of uncertain QOIs. The proposed method is applied to a benchmark electronic packaging design problem. The estimated low-order statistical moments of the QOIs are compared to the results from Monte Carlo simulations to demonstrate the effectiveness of the method. The uncertainty propagation result is then used to facilitate the robust design optimization of the electronic packaging system.

1 INTRODUCTION

With the increasing complexity of engineering systems, *multidisciplinary design optimization* (MDO) has emerged as an important area of research in the context of design optimization and design under uncertainty. Because a complex system often requires analyses in multiple disciplines and/or involves a number of subsystems and components, taking into account the interconnectivities among multiple disciplines in MDO becomes crucial, which raises challenging research issues pertaining to the complexity in simulation, uncertainty quantification, and decision making under uncertainty. Numerous studies have dealt with the various aspects of multidisciplinary analysis, focusing on the development of computational methods [1, 2] as well as applications of these methods to different types of multi-physics interactions [3, 4]. One primary difficulty of MDO stems from the fact that subsystem disciplines are usually coupled so that they can hardly be simulated by their

own.

What makes MDO even more challenging is the consideration of various sources of uncertainties. *Multidisciplinary design under uncertainty* (also called *uncertainty-based multidisciplinary design optimization*, *UMDO* [5]) is a new paradigm for enhancing the reliability and robustness of complex multidisciplinary systems design. Uncertainties can generally be categorized as *aleatory* or *epistemic* [6, 7]; the former represents natural or physical randomness that cannot be controlled or reduced by designers or experimentalists, while the latter refers to uncertainty in the modeling process due to a lack of data and/or a lack of knowledge, which can be fundamentally reduced by gathering more data (experimental and/or computational) and acquiring more knowledge from experts. Kennedy and O'Hagan [8] considered in detail several different sources of uncertainty in model prediction, including: 1) *parametric/input variability* in input variables; 2) *parameter uncertainty* due to naturally fixed but unknown parameters of a simulation model; 3) *model bias* which stems from missing underlying physics; 4) *interpolation uncertainty* that results from having to predict the system response at input combinations that have not been previously simulated; 5) *numerical uncertainty* contributed by numerical implementations of a simulation model; and 6) *experimental variability*. Among the aforementioned categories, (1) and (6) are aleatory, and (2)-(5), which are usually referred to as *model uncertainty*, are epistemic uncertainties. Other types of epistemic uncertainty include uncertainty in the probability distributions (the form and/or parameters of the distribution) of random parameters or random input variables [9].

In the context of design under uncertainty, all types of uncertainties should be considered to assess the uncertainty of system quantities of interest (QOIs). *Uncertainty*

propagation (UP) approaches have been developed in the literature to quantify uncertainty of system QOIs that resides in the simulations. There has been extensive research on uncertainty propagation considering aleatory uncertainty (specifically input variability). *Monte Carlo simulation* (MCS) [10-12] is a straightforward treatment that involves repeated sampling of random input variables and subsequent computer simulations to calculate the statistical moments or the complete probability distribution of system QOIs. Taylor series expansion [13] forms the basis for another class of approaches to approximate the statistical moments of system QOIs based on the sensitivity information of system outputs with respect to input variables. For example, Green et al. [14] applied 1st-order and 2nd-order Taylor expansions in aircraft design; Cao and Duan [15] employed a 1st-order Taylor expansion and convex modeling technique to analyze system output uncertainty. Du et al. extended a first-order reliability method (FORM) to multidisciplinary design with random input variables [16] and interval variables [17]. Many other similar applications can be found in the literature, because Taylor expansion is much more computationally efficient than MCS.

To overcome the computational challenges in multidisciplinary UP, a set of decomposition strategies have been developed to decompose the original problem into a series of disciplinary/subsystem UP problems and consequently enable distributed computing by exploiting the MDO infrastructure. For example, Gu and Renaud implemented an implicit uncertainty propagation method (IUP) for decomposition-based optimization [18] in the scope of robust collaborative optimization [19]; Du and Chen [20, 21] presented a collaborative reliability analysis method to facilitate MPP search; Xiong, et al. [22] developed a multilevel formulation that takes into account response covariance

when setting targets from the higher system level; Sankararaman and Mahadevan [23] developed a likelihood-based approach to remove the interdisciplinary coupling relationship; Liang and Mahadevan [24] introduced a unidirectional decoupling approach. An expanded review of different methods can be found in Yao et al. [5].

In spite of the aforementioned developments, research on uncertainty propagation considering both aleatory uncertainty and epistemic uncertainty has been quite limited. Although certain specific types of epistemic uncertainty have been studied (e.g., incomplete knowledge of the distributions of input variables [9, 25]), model uncertainty, which is an important factor that influences the system prediction, is rarely treated. In fact, combining both uncertainties is not straightforward even in the single-disciplinary context, since there are compound effects between the two as studied by Zhang et al. [26], and analysis under a multidisciplinary system structure is much more intricate. Overall, quantification of model uncertainty in the context of multidisciplinary design is not well explored. Gu et al. [27] proposed a method for worst-case estimation of the system QOIs. Du and Chen [28-30] developed methods for combining input uncertainty and model uncertainty in MDO systems, assuming that a model bias function is predefined. Nevertheless these works did not explicitly quantify model uncertainty. Jiang and Mahadevan [31, 32] developed a Bayesian hierarchical model validation approach to combine lower-level data, higher-level data and computer simulations, but without a direct uncertainty quantification. On the other hand, the lack of prior work on model uncertainty in MDO is also due to the complexity of multidisciplinary analyses, especially in the presence of strong couplings between individual disciplines. Although some research tried to address this issue, the existing methods are developed for specific situations and are not

universal. Sankararaman et al. [33] applied Bayesian networks to analyze the relations between inputs, outputs, and model uncertainty; however, due to the acyclic nature of Bayesian networks, the proposed method cannot deal with feedback couplings or cyclic feed-forward couplings. Allaire et al. [34] specifically considered model bias and interpolation uncertainty using sampling and kernel density estimation for uncertainty assessment; however the sampling-based approach is computationally expensive.

In this paper, we address the aforementioned issues of efficient uncertainty quantification of system QOIs considering both aleatory and epistemic uncertainties. Building on [28, 30], we propose a spatial-random-process (SRP) based multidisciplinary uncertainty analysis (MUA) method in conjunction with disciplinary model uncertainty quantification. SRP modeling [8, 35-42] has been widely used to provide a stochastic representation of model uncertainty that takes into account the difference between computer simulations and physical experiments, as a function of model input variables. The SRP model can be viewed as an emulator to replace the original simulation model and provide updated model prediction, together with uncertainty quantification. Subsequent to SRP disciplinary model uncertainty quantifications, the proposed SRP-based MUA method incorporates the structure of disciplinary SRP emulators to provide compact analytical formulas for assessing low-order statistical moments of the system QOIs. The proposed method first learns the relationship between variations in the linking variables and the input variables, then assesses the variation in the disciplinary outputs, and finally propagates these variations to the system level analysis.

The remainder of the paper is organized as follows: In Section 2, we briefly review basic concepts in SRP modeling and the standard approach to quantifying disciplinary

model uncertainty. Section 3 provides a detailed description of our proposed SRP-based MUA method that utilizes the structure of SRP disciplinary emulators. In Section 4, the proposed MUA method is applied to a benchmark electronic packaging problem. The estimated low-order statistical moments of QOIs are compared to results from MCS to demonstrate the effectiveness of the method. Robust design optimization of an electronic packaging system is then implemented based on the results of the uncertainty propagation. Using the proposed MUA, we achieve a better understanding of the relative impacts on system QOIs from different uncertainty sources in an efficient manner. Conclusions are drawn in Section 5.

2 REVIEW OF SPATIAL-RANDOM-PROCESS (SRP) MODELING & MODEL UNCERTAINTY QUANTIFICATION

Model uncertainty is a significant source of uncertainty that cannot be neglected, since the model predictions will never be in perfect accordance with the true performance. To quantify model uncertainty, computer simulations from a low-fidelity model are first collected, and then compared with data either from physical experiments or high-fidelity simulations when experiments prohibitively expensive. Based on the differences in the response values over the two datasets, the original model is "updated", leading to an emulator (aka. a metamodel, meaning a surrogate model of the original model), and in the process the model uncertainty is quantified. After that, a further validation step ensures validity of the emulator by comparing the emulator to some additional high-fidelity validation data. By iteratively refining the model and/or collecting additional data, the model uncertainty quantification process is performed until the emulator is trust-worthy.

In this section, we briefly review the spatial-random-process (SRP) modeling technique and its applications in two fundamental types of model uncertainty quantification problems: *bias correction*, one that estimates the model bias; and *model calibration*, one that estimates the values of unknown model parameters.

2.1 Spatial-Random-Process (SRP) Modeling

An SRP can be viewed as a collection of random variables distributed over (i.e., indexed by) some spatial domain. *Gaussian process* (GP) models are by far the most common SRP model, and are employed in this research. A GP model for a functional response $f(\cdot)$ is denoted by

$$f(\mathbf{x}) \sim \mathcal{GP}\left(m(\mathbf{x}), V(\mathbf{x}, \mathbf{x}')\right), \tag{1}$$

where $\mathbf{x}=(x_1, \ldots, x_p)$ denotes p-dimensional set of spatial domain variables (i.e., input variables), and $m(\mathbf{x})$ and $V(\mathbf{x},\mathbf{x}')$ are the *mean function* and the *covariance function*, respectively, of the GP. That is, the responses $f(\mathbf{x}^{(1)}), f(\mathbf{x}^{(2)}),\ldots, f(\mathbf{x}^{(n)})$ at any finite set of locations $\mathbf{x}^{(1)}, \mathbf{x}^{(2)},\ldots, \mathbf{x}^{(n)}$ are a collection of random variables that follow a multivariate normal distribution

$$\begin{bmatrix} f(\mathbf{x}^{(1)}) \\ \vdots \\ f(\mathbf{x}^{(n)}) \end{bmatrix} \sim \mathcal{N}\left(\begin{bmatrix} m(\mathbf{x}^{(1)}) \\ \vdots \\ m(\mathbf{x}^{(n)}) \end{bmatrix}, \begin{bmatrix} V(\mathbf{x}^{(1)}, \mathbf{x}^{(1)}) & \cdots & V(\mathbf{x}^{(1)}, \mathbf{x}^{(n)}) \\ \vdots & \ddots & \vdots \\ V(\mathbf{x}^{(n)}, \mathbf{x}^{(1)}) & \cdots & V(\mathbf{x}^{(n)}, \mathbf{x}^{(n)}) \end{bmatrix} \right). \tag{2}$$

SRP models are widely used to emulate various forms of models/functions, especially when original models are too expensive for intensive simulations. The underlying idea is to view the original model/function as a realization of an SRP. The modeling technique follows a three-step procedure. First, a set of data $\mathbf{d}=\{\mathbf{x}_i, f(\mathbf{x}_i), i=1,2,\ldots\}$ is collected at input settings $\mathbf{x}_i$ from the original simulation model. Second, the corresponding SRP is constructed based on the collected data $\mathbf{d}$. Constructing a GP is equivalent to estimating its

mean $m(\mathbf{x})$ and covariance $V(\mathbf{x},\mathbf{x}')$ functions. Typically, one assumes parametric $m(\mathbf{x})$ and $V(\mathbf{x},\mathbf{x}')$ parameterized by a set of hyperparameters $\boldsymbol{\phi}$, and then estimates $\boldsymbol{\phi}$ by maximizing the likelihood function $p(\boldsymbol{\phi}|\mathbf{d})$ using some numerical optimization procedure, which is referred to as *maximum likelihood estimation* (MLE). Common GP parameterizations can be found in [43]. In the last step, predictions can be made at any input settings that have not yet been simulated, by using the existing data and the constructed SRP.

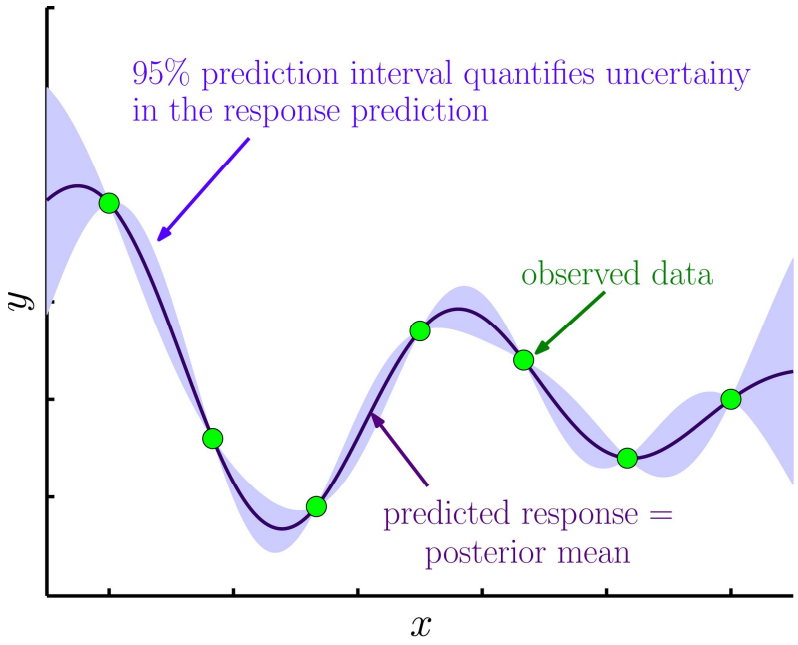

Figure 1. Illustration of SRP modeling

Figure 1 illustrates an SRP emulator of a one-dimensional function $f(x)$. A benefit of using an SRP is that it can quantify the interpolation uncertainty at the locations that have not yet been simulated, represented by the 95% prediction interval depicted by the shaded region. Due to its flexibility and ability to capture the nonlinearity of the underlying simulation model, SRP modeling (primarily GP modeling), has emerged as one of the most popular metamodeling approaches and is applicable for a large variety of different models. The well-known Kriging method [35] is based on GP modeling with linear minimum mean

square error (MMSE) prediction, although Bayesian prediction based on GP modeling is also common. In this work, GP modeling technique will be applied to model different functions, such as the experimental responses, simulation response, etc.

2.2 Model Bias Correction Based on SRP Modeling

As briefly mentioned earlier, bias correction is the process of estimating the model discrepancy. We adopt the following formulation [8, 42, 44-48] that involves the simulation model, experiments, and a *bias function* that represents the difference between simulation and experimental responses:

$$y^e(\mathbf{x}) = y^m(\mathbf{x}) + \delta(\mathbf{x}) + \varepsilon, \tag{3}$$

where $y^e(\mathbf{x})$ denotes the experimental response as a function of the p input variables $\mathbf{x}$, $y^m(\mathbf{x})$ denotes the simulation model response, $\delta(\mathbf{x})$ is the bias function, and ε is a random error accounting for the experimental uncertainty, assumed to be normally, independently distributed as $\mathcal{N}(0,\lambda)$ with unknown variance λ.

Suppose that a set of M simulation response observations $\{\mathbf{x}_i^m, y^m(\mathbf{x}_i^m)\}$ $(i = 1, \dots, M)$ and a set of N experimental response observations $\{\mathbf{x}_i^e, y^e(\mathbf{x}_i^e)\}$ $(i = 1, \dots, N)$ have been collected, which composes the data set $\mathbf{d}$. We represent the simulation model and bias function via the GP models:

$$\begin{aligned} &y^m(\mathbf{x}) \sim \mathcal{GP}\left(\mathbf{h}^m(\mathbf{x})^T\boldsymbol{\beta}^m, V^m(\mathbf{x},\mathbf{x}')\right), \quad V^m(\mathbf{x},\mathbf{x}') = \sigma_m^2 \exp\left\{-\sum_{k=1}^{p}\omega_k^m\left(x_k - x_k'\right)^2\right\}; \\ &\delta(\mathbf{x}) \sim \mathcal{GP}\left(\mathbf{h}^\delta(\mathbf{x})^T\boldsymbol{\beta}^\delta, V^\delta(\mathbf{x},\mathbf{x}')\right), \quad V^\delta(\mathbf{x},\mathbf{x}') = \sigma_\delta^2 \exp\left\{-\sum_{k=1}^{p}\omega_k^\delta\left(x_k - x_k'\right)^2\right\}. \end{aligned} \tag{4}$$

In the above equations, $\mathbf{h}^m(\mathbf{x})$ and $\mathbf{h}^\delta(\mathbf{x})$ denote vector-valued functions whose elements are some prespecified basis functions (e.g., constant, linear, quadratic, etc.), $\boldsymbol{\beta}^m$ and $\boldsymbol{\beta}^\delta$ are two vectors of coefficients associated with $\mathbf{h}^m(\mathbf{x})$ and $\mathbf{h}^\delta(\mathbf{x})$, respectively, σ_m and σ_δ are the prior

standard deviations, and $\boldsymbol{\omega}^m = \left[\omega_1^m, \omega_2^m, \ldots, \omega_p^m\right]^T$ and $\boldsymbol{\omega}^\delta = \left[\omega_1^\delta, \omega_2^\delta, \ldots, \omega_p^\delta\right]^T$ are the spatial correlation parameters used to capture the nonlinearity of the functions. Let $\boldsymbol{\phi} = \{\boldsymbol{\beta}^m, \sigma_m, \boldsymbol{\omega}^m, \boldsymbol{\beta}^\delta, \sigma_\delta, \boldsymbol{\omega}^\delta\}$ denote the collection of unknown hyperparameters that will be estimated via MLE, based on the likelihood function $p(\boldsymbol{\phi}|\mathbf{d})$. Subsequently, we can obtain a prediction of $y^e(\mathbf{x})$ at any untested design of interest $\mathbf{x}$. The prediction equation is (see [42, 43] for full derivation and discussion)

$$\hat{y}^e(\mathbf{x}) = \mathbf{h}(\mathbf{x})\boldsymbol{\beta} + \mathbf{t}(\mathbf{x})\mathbf{V}_\mathbf{d}^{-1}\left(\mathbf{d} - \mathbf{H}\boldsymbol{\beta}\right), \tag{5}$$

where $\hat{y}^e(\mathbf{x})$ is the prediction conditioned on the observed data $\mathbf{d}$ (for notational simplicity we omit the conditioning on $\mathbf{d}$), and

$$\begin{aligned}
\mathbf{V}_\mathbf{d} &= \begin{bmatrix} V^m\left(\mathbf{x}^m, \mathbf{x}^m\right) & V^m\left(\mathbf{x}^e, \mathbf{x}^m\right)^T \\ V^m\left(\mathbf{x}^e, \mathbf{x}^m\right) & V^m\left(\mathbf{x}^e, \mathbf{x}^e\right) + V^\delta\left(\mathbf{x}^e, \mathbf{x}^e\right) + \lambda\mathbf{I} \end{bmatrix}, \\
\mathbf{H} &= \begin{bmatrix} \mathbf{h}^m\left(\mathbf{x}^m\right) & \mathbf{0} \\ \mathbf{h}^m\left(\mathbf{x}^e\right) & \mathbf{h}^\delta\left(\mathbf{x}^e\right) \end{bmatrix}, \quad \mathbf{h}(\mathbf{x}) = \left[\mathbf{h}^m(\mathbf{x}) \quad \mathbf{h}^\delta(\mathbf{x})\right], \\
\mathbf{t}(\mathbf{x}) &= \left[V^m(\mathbf{x}, \mathbf{x}^m) \quad V^m(\mathbf{x}, \mathbf{x}^e) + V^\delta(\mathbf{x}, \mathbf{x}^e)\right], \quad \boldsymbol{\beta} = \left[\boldsymbol{\beta}^m, \boldsymbol{\beta}^\delta\right].
\end{aligned} \tag{6}$$

$\mathbf{I}$ denotes an identity matrix. Here, we are using compact notation with $\mathbf{h}^m(\mathbf{x}^m)$ denoting the matrix $[\mathbf{h}^m(\mathbf{x}_1^m), \mathbf{h}^m(\mathbf{x}_2^m), \ldots, \mathbf{h}^m(\mathbf{x}_M^m)]^T$, and similarly for the other terms. The corresponding prediction mean square error (MSE) is

$$\begin{aligned}
\mathrm{MSE}\left(\hat{y}^e(\mathbf{x})\right) = {} & V^m\left(\mathbf{x}, \mathbf{x}\right) + V^\delta\left(\mathbf{x}, \mathbf{x}\right) + \lambda - \mathbf{t}(\mathbf{x})\mathbf{V}_\mathbf{d}^{-1}\mathbf{t}(\mathbf{x})^T \\
& + \left(\mathbf{h}(\mathbf{x}) - \mathbf{H}^T\mathbf{V}_\mathbf{d}^{-1}\mathbf{t}(\mathbf{x})\right)^T\left(\mathbf{H}^T\mathbf{V}_\mathbf{d}^{-1}\mathbf{H}\right)^{-1}\left(\mathbf{h}(\mathbf{x}) - \mathbf{H}^T\mathbf{V}_\mathbf{d}^{-1}\mathbf{t}(\mathbf{x})\right),
\end{aligned} \tag{7}$$

2.3 Bayesian Model Calibration Based on SRP Modeling

Model calibration is a more comprehensive process that, in addition to considering model bias, also considers the uncertainty associated with unknown model parameters. The

following general model uncertainty quantification formulation has been widely adopted in previous work, for example [8, 38, 40, 49, 50]:

$$y^e(\mathbf{x}) = y^m(\mathbf{x}, \boldsymbol{\theta}^*) + \delta(\mathbf{x}) + \varepsilon, \tag{8}$$

where y^m is now a function of both the design variables $\mathbf{x}$ and an r-dimensional vector $\boldsymbol{\theta}$ of unknown calibration parameters, whose true values are denoted by $\boldsymbol{\theta}^*$.

Data collection from simulations and experiments are conducted similarly to the previous section, although due to the involvement of $\boldsymbol{\theta}$, the collected simulation data are a set of M data points $\{\mathbf{x}_i^m, \boldsymbol{\theta}_i^m, y^m(\mathbf{x}_i^m, \boldsymbol{\theta}_i^m)\}$ $(i = 1, \dots, M)$. Similar to Eq. (4), two GPs can be constructed for the simulation model and the bias function, except that the simulation model is associated with $\boldsymbol{\theta}$:

$$\begin{aligned} &y^m(\mathbf{x}, \boldsymbol{\theta}) \sim \mathcal{GP}\left(\mathbf{h}^m(\mathbf{x}, \boldsymbol{\theta})^T \boldsymbol{\beta}^m, V^m((\mathbf{x}, \boldsymbol{\theta}), (\mathbf{x}', \boldsymbol{\theta}'))\right), \\ &V^m((\mathbf{x}, \boldsymbol{\theta}), (\mathbf{x}', \boldsymbol{\theta}')) = \sigma_m^2 \exp\left\{-\sum_{k=1}^{d} \omega_k^m (x_k - x_k')^2 - \sum_{k=1}^{r} \omega_{d+k}^m (\theta_k - \theta_k')^2\right\}, \end{aligned} \tag{9}$$

With the presence of the calibration parameters $\boldsymbol{\theta}$, it is often not computationally feasible to estimate all the unknown hyperparameters $\boldsymbol{\phi} = \{\boldsymbol{\beta}^m, \sigma_m, \boldsymbol{\omega}^m, \boldsymbol{\beta}^\delta, \sigma_\delta, \boldsymbol{\omega}^\delta\}$ as well as $\boldsymbol{\theta}$ in a single step. Alternatively, a more computationally tractable modular Bayesian treatment [8, 40] was developed to handle the computational challenges. One first specifies a prior probability distribution $p(\boldsymbol{\theta})$ of the calibration parameters $\boldsymbol{\theta}$ based on past experience and/or expert opinion, covering a range over which the true values of $\boldsymbol{\theta}$ are likely to lie. Then the likelihood function [marginalized with respect to $p(\boldsymbol{\theta})$] is maximized to obtain the MLE of $\boldsymbol{\phi}$. Based on Bayes theorem, the posterior distribution of $\boldsymbol{\theta}$ is $p(\boldsymbol{\theta}|\mathbf{d}, \boldsymbol{\phi}) \propto p(\boldsymbol{\phi}|\mathbf{d}, \boldsymbol{\theta}) p(\boldsymbol{\theta})$, where $p(\boldsymbol{\phi}|\mathbf{d}, \boldsymbol{\theta})$ is the value of likelihood function at different $\boldsymbol{\theta}$ values. The model prediction (defined as the posterior mean) and MSE (defined as the posterior variance),

conditioned on a specified value of $\boldsymbol{\theta}$, can be obtained via:

$$\begin{aligned}
&\hat{y}^e(\mathbf{x},\boldsymbol{\theta}) = \mathbf{h}(\mathbf{x},\boldsymbol{\theta})\boldsymbol{\beta} + \mathbf{t}(\mathbf{x},\boldsymbol{\theta})\mathbf{V}_\mathbf{d}(\boldsymbol{\theta})^{-1}\left(\mathbf{d} - \mathbf{H}(\boldsymbol{\theta})\boldsymbol{\beta}\right), \\
&\mathrm{MSE}\left(\hat{y}^e(\mathbf{x},\boldsymbol{\theta})\right) = V^m\left((\mathbf{x},\boldsymbol{\theta}),(\mathbf{x},\boldsymbol{\theta})\right) + V^\delta\left(\mathbf{x},\mathbf{x}\right) + \lambda - \mathbf{t}(\mathbf{x},\boldsymbol{\theta})\mathbf{V}_\mathbf{d}(\boldsymbol{\theta})^{-1}\mathbf{t}(\mathbf{x},\boldsymbol{\theta})^T \\
&\qquad + \left(\mathbf{h}(\mathbf{x},\boldsymbol{\theta}) - \mathbf{H}(\boldsymbol{\theta})^T\mathbf{V}_\mathbf{d}(\boldsymbol{\theta})^{-1}\mathbf{t}(\mathbf{x},\boldsymbol{\theta})\right)^T\left(\mathbf{H}(\boldsymbol{\theta})^T\mathbf{V}_\mathbf{d}(\boldsymbol{\theta})^{-1}\mathbf{H}(\boldsymbol{\theta})\right)^{-1} \\
&\qquad \times\left(\mathbf{h}(\mathbf{x},\boldsymbol{\theta}) - \mathbf{H}(\boldsymbol{\theta})^T\mathbf{V}_\mathbf{d}(\boldsymbol{\theta})^{-1}\mathbf{t}(\mathbf{x},\boldsymbol{\theta})\right).
\end{aligned} \tag{10}$$

Notice that Eq. (10) is very similar to Eqs. (5) and (7), aside from the additional dependence on $\boldsymbol{\theta}$. To calculate the marginal (i.e., unconditional) prediction $\hat{y}^e(\mathbf{x})$ of the experimental response, we marginalize the conditional prediction (10) with respect to the posterior distribution $p(\boldsymbol{\theta}|\mathbf{d},\boldsymbol{\phi})$ of the calibration parameters. Details can be found in [8, 40], and the final equations will be revisited in Section 3.

The SRP-based approach for model uncertainty quantification, whether bias correction or model calibration, has the merit of providing a prediction variance, in addition to a prediction mean. SRP modeling technique brings together the simulations and experiments and offers a tractable way to evaluate the relationship between them as well as between the spatial locations. The MSE terms in Eqs. (7) and (10) are comprehensive by including these relationships, and provide information on the extent to which the experimental response may differ from their predicted values. Here, the source of the prediction variance is not the variability of the input variables, since only fixed, nonrandom input variables were included in those models. Instead, the sources of uncertainty are the model bias function, the experimental variability, and the unknown calibration parameters. If desired, an expression for the uncertainty in the bias function $\delta(\mathbf{x})$ can also be produced in a similar manner.

In the next section, the SRP-based approach will be applied to quantifying disciplinary model uncertainty in a multidisciplinary system. The method requires a reasonable amount of high-fidelity data at the disciplinary/component level, rather than at the whole system level.

3 MULTIDISCIPLINARY SYSTEM UNCERTAINTY PROPAGATION WITH ALEATORY AND EPESTEMIC UNCERTAINTIES

A notional multilevel multidisciplinary system is depicted in **Figure 2**. A typical MDO system involves individual disciplinary input variables $\mathbf{x}_{\text{ind}}=\{\mathbf{x}_i, i=1, \ldots, ND\}$ (with ND as the number of disciplines), and shared input variables $\mathbf{x}_s$ across at least two disciplines. The disciplines are coupled via linking variables $\mathbf{u}_{ij}$, which represent the outputs from the ith discipline that also serve as inputs for the jth discipline. If both $\mathbf{u}_{ij}$ and $\mathbf{u}_{ji}$ are nonempty, the relation between the ith and jth disciplines is referred to as *feedback* coupling; otherwise it is *feed-forward* coupling. The system QOIs $\mathbf{y}_{\text{sys}}$ are linked to disciplinary responses $\mathbf{y}_{\text{ind}}=\{\mathbf{y}_i, i=1, \ldots, ND\}$ through the system analysis model. Beyond existing work that mostly considers only the (aleatory) input variability (blocks A in **Figure 2**), this research will also consider epistemic model uncertainty (blocks B in **Figure 2**).

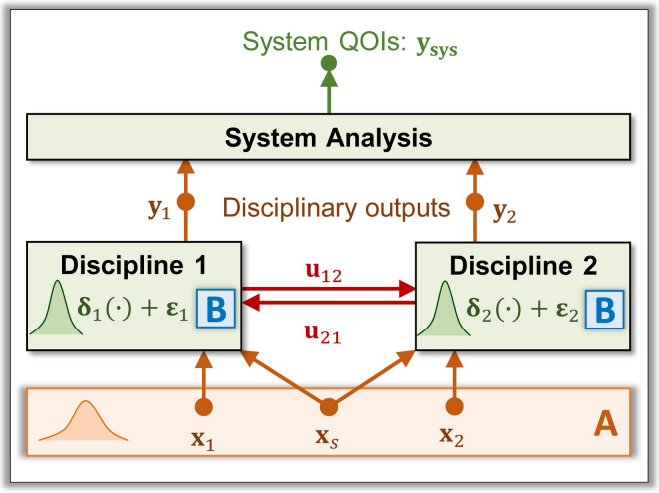

Figure 2. A notional multidisciplinary system and its possible sources of uncertainties: Block A. input variability (aleatory); Block B. model uncertainty (epistemic)

As mentioned in the introduction, Du and Chen [28, 30] developed a *system uncertainty analysis* (SUA) method to estimate the mean and variance of system performance subject to uncertainties associated with both input variables and design models. A specific model bias formulation was assumed such that the true response is equal to the sum of the original model and a stochastic bias function, whose mean and variance are known at any input setting. The 1st-order Taylor expansion is then applied to estimate the means and variances of linking variables and disciplinary output variables, respectively, in sequence. However, the original SUA is limited in four respects: 1) It does not consider comprehensively all possible sources of uncertainty. For example, the experimental variability is overlooked. 2) It does not provide physical justification of the predefined bias function. 3) It requires new simulation data when applying the approach, which may not be affordable because the disciplinary simulation models are often computationally expensive. 4) It only evaluates the mean and variance of the QOIs, but neglects their covariance, which is critical in multidisciplinary design. In order to overcome these drawbacks, we develop a SRP-based multidisciplinary uncertainty analysis (MUA) method,

which builds on the basic idea of the original SUA but derives analytical formulae by incorporating the structure of the SRP models introduced in Section 2.

The SRP-based MUA procedure is shown in **Figure 3**. For each individual discipline, model uncertainty quantification is conducted (either model bias correction or model calibration, as described in Section 2) by incorporating disciplinary experimental and simulation data. After that, given a specific input setting (including the mean and covariance of disciplinary and shared input variables), we evaluate the means of all linking variables ($\mathbf{u}_{ij}$'s) and disciplinary outputs ($\mathbf{y}_{\text{ind}}$) (Section 3.1), and the covariances of linking variables (Section 3.2) and of disciplinary outputs (Section 3.3), all in the context of the coupled multidisciplinary system. From these, the uncertainty in the system QOIs ($\mathbf{y}_{\text{sys}}$) can be calculated.

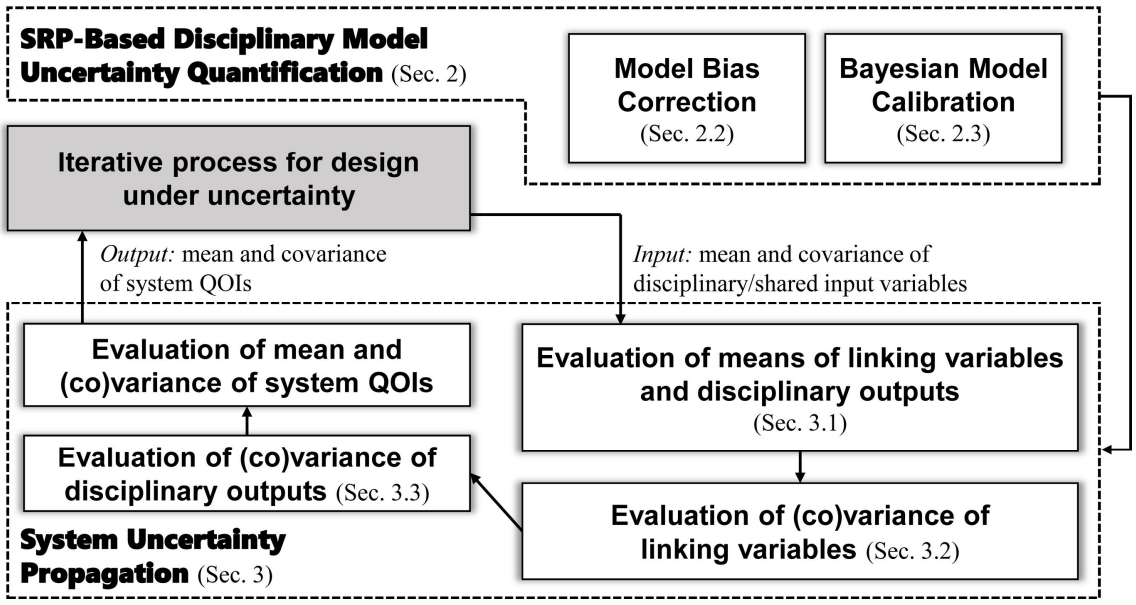

Figure 3. The procedure of the proposed SRP-based MUA method

The means and covariances are posterior in the sense that they are conditioned on the collected data (**d** in Table 1, below), and they are with respect to aleatory uncertainty in the

inputs $\mathbf{x}_{\text{ind}}$ and $\mathbf{x}_s$ (and any uncertainty that induces in the linking variables) and epistemic uncertainty as quantified in the process of calibration and bias correction of the individual disciplinary emulators. The mean and covariance expressions that we derive are noteworthy, in that they allow the multidisciplinary system level output uncertainty to be conveniently quantified, using only the individual disciplinary emulators. That is, one does not have to conduct the system level simulation, which may be extremely computationally expensive or even impossible. Within the framework of design under uncertainty, the process will be iterative by continuously assigning different input settings and evaluating the mean and covariance of system QOIs.

3.1 Evaluation of Means of Linking Variables and Disciplinary Outputs

By inspection of Eqs. (5), (7) and (10), we can write the prediction of experimental responses in the following form (which applies to either the disciplinary outputs or the linking variables):

$$y^e(\mathbf{x}) = \hat{y}^e(\mathbf{x}) + Z(\mathbf{x}), \tag{11}$$

where $\hat{y}^e(\mathbf{x})$ denotes the mean prediction after uncertainty quantification (i.e., the emulator after bias correction and calibration), and $Z(\mathbf{x})$ is defined as the prediction error $y^e(\mathbf{x}) - \hat{y}^e(\mathbf{x})$. From the SRP modeling results in Sections 2.2 and 2.3, $Z(\mathbf{x})$ is a zero-mean random variable with variance denoted by $\sigma_Z^2(\mathbf{x})$. Note that this is the resulting equation *after* model uncertainty quantification. Comparing Eq. (11) with Eqs. (3) and (8) (which are the SRP models *before* model uncertainty quantification), the mean prediction $\hat{y}^e(\mathbf{x})$ encompasses the estimation / prediction of the bias function $\delta(\mathbf{x})$ and the unknown parameters $\boldsymbol{\theta}$, and the random term $Z(\mathbf{x})$ accounts for the uncertainty in the prediction. The equations for calculating $\hat{y}^e(\mathbf{x})$ and $\sigma_Z^2(\mathbf{x})$ are summarized in **Table 1**. Mathematically,

$\sigma_Z^2(\mathbf{x})$ is equivalent to $\mathrm{MSE}\left(\hat{y}^e(\mathbf{x})\right)$.

Applying Eq. (11) to the MDO system, we can write the predictions of the linking variables and the disciplinary output variables respectively as (for i=1, 2, …, ND):

$$\mathbf{u}_{i\cdot}^e(\mathbf{x}_i,\mathbf{x}_s,\mathbf{u}_{\cdot i}^e)=\hat{\mathbf{u}}_{i\cdot}^e(\mathbf{x}_i,\mathbf{x}_s,\mathbf{u}_{\cdot i}^e)+\mathbf{Z}_{ui\cdot}(\mathbf{x}_i,\mathbf{x}_s,\mathbf{u}_{\cdot i}^e), \tag{12}$$

and

$$\mathbf{y}_i^e(\mathbf{x}_i,\mathbf{x}_s,\mathbf{u}_{\cdot i}^e)=\hat{\mathbf{y}}_i^e(\mathbf{x}_i,\mathbf{x}_s,\mathbf{u}_{\cdot i}^e)+\mathbf{Z}_{yi}(\mathbf{x}_i,\mathbf{x}_s,\mathbf{u}_{\cdot i}^e), \tag{13}$$

where $\mathbf{u}_{i\cdot}$ denotes all linking variables output from the ith discipline, and $\mathbf{u}_{\cdot i}$ denotes all linking variables input to the ith discipline. Same as Eq. (11), the superscript "e" refers to the experimental response, and the hat "^" notation refers to the mean prediction of the experimental response. The terms $\hat{\mathbf{u}}_{i\cdot}^e(\cdot,\cdot,\cdot), \hat{\mathbf{y}}_i^e(\cdot,\cdot,\cdot), \mathbf{Z}_{ui\cdot}(\cdot,\cdot,\cdot), \mathbf{Z}_{yi}(\cdot,\cdot,\cdot)$ in above equations can be calculated by applying the equations in **Table 1** to data from individual disciplines. One should view $\hat{\mathbf{u}}_{i\cdot}^e(\cdot,\cdot,\cdot)$ and $\hat{\mathbf{y}}_i^e(\cdot,\cdot,\cdot)$ as functions that are given by the calibrated and bias-corrected emulators produced from the **Table 1** calculations.

Table 1. Equations for calculating $\hat{y}^e(\mathbf{x})$ and $\sigma_Z^2(\mathbf{x})$ from uncertainty quantification

$y^e(\mathbf{x})=\hat{y}^e(\mathbf{x})+Z(\mathbf{x}),\quad E\left[Z(\mathbf{x})\middle\vert\mathbf{x}\right]=0,\quad Var\left[Z(\mathbf{x})\middle\vert\mathbf{x}\right]=\sigma_Z^2(\mathbf{x})$	
Bias Correction	$\hat{y}^e(\mathbf{x})=\mathbf{h}(\mathbf{x})\boldsymbol{\beta}+\mathbf{t}(\mathbf{x})\mathbf{V}_\mathbf{d}^{-1}\left(\mathbf{d}-\mathbf{H}\boldsymbol{\beta}\right),$ $\sigma_Z^2(\mathbf{x})=V^m\left(\mathbf{x},\mathbf{x}\right)+V^\delta\left(\mathbf{x},\mathbf{x}\right)+\lambda-\mathbf{t}(\mathbf{x})\mathbf{V}_\mathbf{d}^{-1}\mathbf{t}(\mathbf{x})^T$ $+\left(\mathbf{h}(\mathbf{x})-\mathbf{H}^T\mathbf{V}_\mathbf{d}^{-1}\mathbf{t}(\mathbf{x})\right)^T\left(\mathbf{H}^T\mathbf{V}_\mathbf{d}^{-1}\mathbf{H}\right)^{-1}\left(\mathbf{h}(\mathbf{x})-\mathbf{H}^T\mathbf{V}_\mathbf{d}^{-1}\mathbf{t}(\mathbf{x})\right).$
Model Calibration	$\hat{y}^e(\mathbf{x})=\int\left[\mathbf{h}(\mathbf{x},\boldsymbol{\theta})\boldsymbol{\beta}+\mathbf{t}(\mathbf{x},\boldsymbol{\theta})\mathbf{V}_\mathbf{d}(\boldsymbol{\theta})^{-1}\left(\mathbf{d}-\mathbf{H}(\boldsymbol{\theta})\boldsymbol{\beta}\right)\right]p(\boldsymbol{\theta}\vert\mathbf{d},\boldsymbol{\phi})\mathrm{d}\boldsymbol{\theta},$ $\sigma_Z^2(\mathbf{x})=\int\left[V^m\left((\mathbf{x},\boldsymbol{\theta}),(\mathbf{x},\boldsymbol{\theta})\right)+V^\delta\left(\mathbf{x},\mathbf{x}\right)+\lambda-\mathbf{t}(\mathbf{x},\boldsymbol{\theta})\mathbf{V}_\mathbf{d}(\boldsymbol{\theta})^{-1}\mathbf{t}(\mathbf{x},\boldsymbol{\theta})^T\right.$ $+\left(\mathbf{h}(\mathbf{x},\boldsymbol{\theta})-\mathbf{H}(\boldsymbol{\theta})^T\mathbf{V}_\mathbf{d}(\boldsymbol{\theta})^{-1}\mathbf{t}(\mathbf{x},\boldsymbol{\theta})\right)^T\left(\mathbf{H}(\boldsymbol{\theta})^T\mathbf{V}_\mathbf{d}(\boldsymbol{\theta})^{-1}\mathbf{H}(\boldsymbol{\theta})\right)^{-1}$ $\left.\times\left(\mathbf{h}(\mathbf{x},\boldsymbol{\theta})-\mathbf{H}(\boldsymbol{\theta})^T\mathbf{V}_\mathbf{d}(\boldsymbol{\theta})^{-1}\mathbf{t}(\mathbf{x},\boldsymbol{\theta})\right)\right]p(\boldsymbol{\theta}\vert\mathbf{d},\boldsymbol{\phi})\mathrm{d}\boldsymbol{\theta}.$

Given the information that the individual input variables $\mathbf{x}_{\mathrm{ind}}$ are randomly distributed

with mean $\boldsymbol{\mu}_x$, and that the shared input variables $\mathbf{x}_s$ are randomly distributed with mean $\boldsymbol{\mu}_{xs}$, to calculate the means of the linking variables and disciplinary outputs, we use a 1st-order Taylor expansion of $\hat{\mathbf{u}}_{i\cdot}^{e}(\cdot,\cdot,\cdot)$ and $\hat{\mathbf{y}}_{i}^{e}(\cdot,\cdot,\cdot)$ in Eqs. (12)~(13) about the mean values of the input variables and linking variables, which yields (i=1, …, ND)

$$\begin{aligned}\mathbf{u}_{i\cdot}^{e}(\mathbf{x}_i,\mathbf{x}_s,\mathbf{u}_{\cdot i}^{e}) \approx \hat{\mathbf{u}}_{i\cdot}^{e}(\boldsymbol{\mu}_{xi},\boldsymbol{\mu}_{xs},\boldsymbol{\mu}_{u\cdot i}) + \sum_{j=1,j\neq i}^{ND}\frac{\partial\hat{\mathbf{u}}_{i\cdot}^{e}}{\partial\mathbf{u}_{j\cdot}^{e}}\left(\mathbf{u}_{j\cdot}^{e}-\boldsymbol{\mu}_{uj\cdot}\right)\\ +\frac{\partial\hat{\mathbf{u}}_{i\cdot}^{e}}{\partial\mathbf{x}_s}\left(\mathbf{x}_s-\boldsymbol{\mu}_{xs}\right)+\frac{\partial\hat{\mathbf{u}}_{i\cdot}^{e}}{\partial\mathbf{x}_i}\left(\mathbf{x}_i-\boldsymbol{\mu}_{xi}\right)+\mathbf{Z}_{ui\cdot}(\mathbf{x}_i,\mathbf{x}_s,\mathbf{u}_{\cdot i}^{e}),\end{aligned} \tag{14}$$

and

$$\begin{aligned}\mathbf{y}_{i}^{e}(\mathbf{x}_i,\mathbf{x}_s,\mathbf{u}_{\cdot i}^{e}) \approx \hat{\mathbf{y}}_{i}^{e}(\boldsymbol{\mu}_{xi},\boldsymbol{\mu}_{xs},\boldsymbol{\mu}_{u\cdot i}) + \sum_{j=1,j\neq i}^{ND}\frac{\partial\hat{\mathbf{y}}_{i}^{e}}{\partial\mathbf{u}_{j\cdot}^{e}}\left(\mathbf{u}_{j\cdot}^{e}-\boldsymbol{\mu}_{uj\cdot}\right)\\ +\frac{\partial\hat{\mathbf{y}}_{i}^{e}}{\partial\mathbf{x}_s}\left(\mathbf{x}_s-\boldsymbol{\mu}_{xs}\right)+\frac{\partial\hat{\mathbf{y}}_{i}^{e}}{\partial\mathbf{x}_i}\left(\mathbf{x}_i-\boldsymbol{\mu}_{xi}\right)+\mathbf{Z}_{yi}(\mathbf{x}_i,\mathbf{x}_s,\mathbf{u}_{\cdot i}^{e}),\end{aligned} \tag{15}$$

where $\boldsymbol{\mu}_{ui\cdot}$ denotes the mean of $\mathbf{u}_{i\cdot}$, $\boldsymbol{\mu}_{u\cdot i}$ denotes the mean of $\mathbf{u}_{\cdot i}$, and $\boldsymbol{\mu}_{yi}$ denotes the mean of $\mathbf{y}_i$. Many of $\partial\hat{\mathbf{u}}_{i\cdot}^{e}/\partial\mathbf{u}_{j\cdot}^{e}$ and $\partial\hat{\mathbf{y}}_{i}^{e}/\partial\mathbf{u}_{j\cdot}^{e}$ will be zero, if $\mathbf{u}_{j\cdot}^{e}$ does not include $\mathbf{u}_{\cdot i}^{e}$. Notice that in the above equations, $\mathbb{E}\left[\mathbf{u}_{j\cdot}^{e}-\boldsymbol{\mu}_{uj\cdot}\right]=\mathbf{0}$, $\mathbb{E}[\mathbf{x}_s-\boldsymbol{\mu}_{xs}]=\mathbf{0}$, and $\mathbb{E}[\mathbf{x}_i-\boldsymbol{\mu}_{xi}]=\mathbf{0}$ for any i and j, by definition. Moreover, all $\mathbf{Z}$ quantities are zero mean, as a property of the GP predictors and prediction errors. Therefore, taking the expectation of both sides in Eqs. (14)~(15), we can approximate the means of the linking variables and disciplinary outputs for the ith discipline by solving the simultaneous equations:

$$\boldsymbol{\mu}_{ui\cdot}\approx\hat{\mathbf{u}}_{i\cdot}^{e}(\boldsymbol{\mu}_{xi},\boldsymbol{\mu}_{xs},\boldsymbol{\mu}_{u\cdot i}), \tag{16}$$

$$\boldsymbol{\mu}_{yi}\approx\hat{\mathbf{y}}_{i}^{e}(\boldsymbol{\mu}_{xi},\boldsymbol{\mu}_{xs},\boldsymbol{\mu}_{u\cdot i}). \tag{17}$$

These equations are valid if the input variances are small enough that the emulators $\hat{\mathbf{u}}_{i\cdot}^{e}(\cdot,\cdot,\cdot)$ and $\hat{\mathbf{y}}_{i}^{e}(\cdot,\cdot,\cdot)$ in Eqs. (12) and (13) are approximately linear over the range of input

variation. These assumptions are also required for the covariance calculations later in this section. Solving the equations simultaneously for all disciplines requires only a computationally efficient system level analysis using the individually bias corrected/calibrated emulators from Section 2. It does not require a system level simulation.

3.2 Evaluation of (Co)Variance of Linking Variables

Let $\mathbf{X} = [\mathbf{x}_s^T, \mathbf{x}_{\text{ind}}^T]^T$ denote the vector of all the shared input variables $\mathbf{x}_s$ and the individual input variables $\mathbf{x}_{\text{ind}}$, collectively. In order to calculate the covariance matrix of the linking variables (i.e., all $\mathbf{u}$'s), we rewrite Eq. (14) by collecting all $\mathbf{u}$ terms on the left hand side, i.e.,

$$\mathbf{A}(\mathbf{u}^e - \boldsymbol{\mu}_u) \approx \mathbf{B}(\mathbf{X} - \boldsymbol{\mu}_X) + \mathbf{Z}_u, \tag{18}$$

where

$$\mathbf{u}^e = \left[\left(\mathbf{u}_{1\cdot}^e\right)^T \quad \cdots \quad \left(\mathbf{u}_{ND\cdot}^e\right)^T \right]^T, \quad \boldsymbol{\mu}_u = \left[\left(\boldsymbol{\mu}_{u1\cdot}\right)^T \quad \cdots \quad \left(\boldsymbol{\mu}_{uND\cdot}\right)^T \right]^T,$$

$$\boldsymbol{\mu}_X = \left[\left(\boldsymbol{\mu}_{xs}\right)^T \;\middle|\; \left(\boldsymbol{\mu}_{x1}\right)^T \quad \cdots \quad \left(\boldsymbol{\mu}_{xND}\right)^T \right]^T, \quad \mathbf{Z}_u = \left[\mathbf{Z}_{u1\cdot}^T \quad \cdots \quad \mathbf{Z}_{uND\cdot}^T \right]^T,$$

$$\mathbf{A} = \begin{bmatrix} \mathbf{I} & -\dfrac{\partial \hat{\mathbf{u}}_{1\cdot}^e}{\partial \mathbf{u}_{2\cdot}^e} & \cdots & -\dfrac{\partial \hat{\mathbf{u}}_{1\cdot}^e}{\partial \mathbf{u}_{ND\cdot}^e} \\ -\dfrac{\partial \hat{\mathbf{u}}_{2\cdot}^e}{\partial \mathbf{u}_{1\cdot}^e} & \mathbf{I} & \cdots & -\dfrac{\partial \hat{\mathbf{u}}_{2\cdot}^e}{\partial \mathbf{u}_{ND\cdot}^e} \\ \vdots & \vdots & \ddots & \vdots \\ -\dfrac{\partial \hat{\mathbf{u}}_{ND\cdot}^e}{\partial \mathbf{u}_{1\cdot}^e} & -\dfrac{\partial \hat{\mathbf{u}}_{ND\cdot}^e}{\partial \mathbf{u}_{2\cdot}^e} & \cdots & \mathbf{I} \end{bmatrix}, \quad \mathbf{B} = \left[\begin{array}{c|ccc} \dfrac{\partial \hat{\mathbf{u}}_{1\cdot}^e}{\partial \mathbf{x}_s} & \dfrac{\partial \hat{\mathbf{u}}_{1\cdot}^e}{\partial \mathbf{x}_1} & \mathbf{0} & \cdots & \mathbf{0} \\ \dfrac{\partial \hat{\mathbf{u}}_{2\cdot}^e}{\partial \mathbf{x}_s} & \mathbf{0} & \dfrac{\partial \hat{\mathbf{u}}_{2\cdot}^e}{\partial \mathbf{x}_2} & \cdots & \mathbf{0} \\ \vdots & \vdots & \vdots & \ddots & \vdots \\ \dfrac{\partial \hat{\mathbf{u}}_{ND\cdot}^e}{\partial \mathbf{x}_s} & \mathbf{0} & \mathbf{0} & \cdots & \dfrac{\partial \hat{\mathbf{u}}_{ND\cdot}^e}{\partial \mathbf{x}_{ND}} \end{array}\right].$$

In the preceding, $\boldsymbol{\mu}_X$ and $\boldsymbol{\mu}_u$ denote the mean vectors for $\mathbf{X}$ and $\mathbf{u}^e$, respectively. Notice that all the entries in the matrices $\mathbf{A}$ and $\mathbf{B}$ have analytical forms that can be directly calculated from the uncertainty quantification equations in **Table 1**. Using bias correction as an example to illustrate the calculations, we have

$$\begin{aligned}
\frac{\partial \hat{\mathbf{u}}_{i\cdot}^{e}}{\partial \mathbf{u}_{j\cdot}^{e}} &= \frac{\partial \mathbf{h}_{ui\cdot}}{\partial \mathbf{u}_{j\cdot}^{e}}\boldsymbol{\beta}_{ui\cdot} + \frac{\partial \mathbf{t}_{ui\cdot}}{\partial \mathbf{u}_{j\cdot}^{e}}\mathbf{V}_{\mathbf{d}ui\cdot}^{-1}\left(\mathbf{d}_{ui\cdot} - \mathbf{H}_{ui\cdot}\boldsymbol{\beta}_{ui\cdot}\right), \quad i,j = 1,\ldots,ND; i \neq j; \\
\frac{\partial \hat{\mathbf{u}}_{i\cdot}^{e}}{\partial \mathbf{x}_{j}} &= \frac{\partial \mathbf{h}_{ui\cdot}}{\partial \mathbf{x}_{j}}\boldsymbol{\beta}_{ui\cdot} + \frac{\partial \mathbf{t}_{ui\cdot}}{\partial \mathbf{x}_{j}}\mathbf{V}_{\mathbf{d}ui\cdot}^{-1}\left(\mathbf{d}_{ui\cdot} - \mathbf{H}_{ui\cdot}\boldsymbol{\beta}_{ui\cdot}\right), \quad i = 1,\ldots,ND; j = 1,\ldots,ND, s;
\end{aligned} \tag{19}$$

where the symbols $\mathbf{h}_{ui\cdot}$, $\mathbf{t}_{ui\cdot}$, $\mathbf{V}_{\mathbf{d}ui\cdot}$, $\mathbf{d}_{ui\cdot}$, $\mathbf{H}_{ui\cdot}$, $\boldsymbol{\beta}_{ui\cdot}$ all denote quantities from the uncertainty quantification in **Table 1**. Eq. (18) becomes

$$\mathbf{u}^{e} - \boldsymbol{\mu}_{u} \approx \mathbf{A}^{-1}\mathbf{B}(\mathbf{X} - \boldsymbol{\mu}_{X}) + \mathbf{A}^{-1}\mathbf{Z}_{u}, \tag{20}$$

from which it follows that the covariance matrix of linking variables is

$$\begin{aligned}
\boldsymbol{\Sigma}_{u} \approx\ & (\mathbf{A}^{-1}\mathbf{B})\boldsymbol{\Sigma}_{X}(\mathbf{A}^{-1}\mathbf{B})^{T} + (\mathbf{A}^{-1})\boldsymbol{\Sigma}_{Zu}(\mathbf{A}^{-1})^{T} \\
& + (\mathbf{A}^{-1}\mathbf{B})\boldsymbol{\Sigma}_{X,Zu}(\mathbf{A}^{-1})^{T} + (\mathbf{A}^{-1})\boldsymbol{\Sigma}_{X,Zu}^{T}(\mathbf{A}^{-1}\mathbf{B})^{T},
\end{aligned} \tag{21}$$

where $\boldsymbol{\Sigma}_{u}$, $\boldsymbol{\Sigma}_{X}$ and $\boldsymbol{\Sigma}_{Zu}$ denote the covariance matrices of $\mathbf{u}^{e}$, $\mathbf{X}$, and $\mathbf{Z}_{u}$, respectively. $\boldsymbol{\Sigma}_{X,Zu}$ denotes the cross-covariance matrix of $\mathbf{X}$ and $\mathbf{Z}_{u}$, which, according to the law of iterated expectations, is

$$\begin{aligned}
\boldsymbol{\Sigma}_{X,Zu} &= \mathbb{E}\left[(\mathbf{X} - \boldsymbol{\mu}_{X})\mathbf{Z}_{u}^{T}\right] = \mathbb{E}\left[\mathbb{E}\left[(\mathbf{X} - \boldsymbol{\mu}_{X})\mathbf{Z}_{u}^{T}\middle|\mathbf{X}\right]\right] \\
&= \mathbb{E}\left[(\mathbf{X} - \boldsymbol{\mu}_{X})\mathbb{E}\left[\mathbf{Z}_{u}^{T}\middle|\mathbf{X}\right]\right] = \mathbb{E}\left[(\mathbf{X} - \boldsymbol{\mu}_{X})\cdot\mathbf{0}\right] = \mathbf{0}.
\end{aligned} \tag{22}$$

Consequently, Eq. (21) becomes

$$\boldsymbol{\Sigma}_{u} \approx (\mathbf{A}^{-1}\mathbf{B})\boldsymbol{\Sigma}_{X}(\mathbf{A}^{-1}\mathbf{B})^{T} + (\mathbf{A}^{-1})\boldsymbol{\Sigma}_{Zu}(\mathbf{A}^{-1})^{T}. \tag{23}$$

The covariance of the linking variables represented by Eq. (23) stems from both the variation of input variables (represented by $\boldsymbol{\Sigma}_{X}$) and the model uncertainty (represented by $\boldsymbol{\Sigma}_{Zu}$). Practically to calculate $\boldsymbol{\Sigma}_{Zu}$, we assume in this paper that the epistemic uncertainty of each individual disciplinary model is quantified separately, and that the elements of $\mathbf{Z}_{u}$ are uncorrelated with each other. That is, we approximate $\boldsymbol{\Sigma}_{Zu} = \mathrm{diag}(\sigma_{Zu1\cdot}^{2}, \ldots, \sigma_{ZuND\cdot}^{2})$ as a diagonal matrix with ith diagonal element (i=1, …, ND) given by

$$\begin{aligned}\sigma^2_{Zui\cdot} &= \mathbb{E}\Big[\mathrm{Var}\Big[\mathbf{Z}_{ui\cdot}\Big|\mathbf{x}_i,\mathbf{x}_s,\mathbf{u}^e_{\cdot i}\Big]\Big]+\mathrm{Var}\Big[\mathbb{E}\Big[\mathbf{Z}_{ui\cdot}\Big|\mathbf{x}_i,\mathbf{x}_s,\mathbf{u}^e_{\cdot i}\Big]\Big]\\ &= \mathbb{E}\Big[\mathrm{Var}\Big[\mathbf{Z}_{ui\cdot}\Big|\mathbf{x}_i,\mathbf{x}_s,\mathbf{u}^e_{\cdot i}\Big]\Big]\approx\sigma^2_{Zui\cdot}(\boldsymbol{\mu}_{xi},\boldsymbol{\mu}_{xs},\boldsymbol{\mu}_{u\cdot i}),\end{aligned} \tag{24}$$

which, again, can be directly calculated from the uncertainty quantification equations in **Table 1**. Note that this is not the same as assuming the linking variables **u** to be uncorrelated with each other; rather, we are only assuming that the *errors* (after model uncertainty quantification) in predicting the linking variables are uncorrelated.

3.3 Evaluation of (Co)Variance of Disciplinary Outputs

Proceeding as in the previous section, the Taylor series expansion (15) for the subsystem outputs results in the approximation

$$\begin{aligned}\mathbf{y}^e-\boldsymbol{\mu}_y &\approx \mathbf{E}(\mathbf{u}^e-\boldsymbol{\mu}_u)+\mathbf{F}(\mathbf{X}-\boldsymbol{\mu}_X)+\mathbf{Z}_y\\ &= \left(\mathbf{E}\mathbf{A}^{-1}\mathbf{B}+\mathbf{F}\right)(\mathbf{X}-\boldsymbol{\mu}_X)+\mathbf{E}\mathbf{A}^{-1}\mathbf{Z}_u+\mathbf{Z}_y,\end{aligned} \tag{25}$$

where

$$\mathbf{y}^e=\left[\left(\mathbf{y}^e_1\right)^T\ \cdots\ \left(\mathbf{y}^e_{ND}\right)^T\right]^T,\quad \boldsymbol{\mu}_y=\left[\left(\boldsymbol{\mu}_{y1}\right)^T\ \cdots\ \left(\boldsymbol{\mu}_{yND}\right)^T\right]^T,\quad \mathbf{Z}_y=\left[\mathbf{Z}^T_{y1}\ \cdots\ \mathbf{Z}^T_{yND}\right]^T,$$

$$\mathbf{E}=\begin{bmatrix}\mathbf{0} & \frac{\partial\hat{\mathbf{y}}^e_1}{\partial\mathbf{u}^e_{2\cdot}} & \cdots & \frac{\partial\hat{\mathbf{y}}^e_1}{\partial\mathbf{u}^e_{ND\cdot}}\\ \frac{\partial\hat{\mathbf{y}}^e_2}{\partial\mathbf{u}^e_{1\cdot}} & \mathbf{0} & \cdots & \frac{\partial\hat{\mathbf{y}}^e_2}{\partial\mathbf{u}^e_{ND\cdot}}\\ \vdots & \vdots & \ddots & \vdots\\ \frac{\partial\hat{\mathbf{y}}^e_{ND}}{\partial\mathbf{u}^e_{1\cdot}} & \frac{\partial\hat{\mathbf{y}}^e_{ND}}{\partial\mathbf{u}^e_{2\cdot}} & \cdots & \mathbf{0}\end{bmatrix},\quad \mathbf{F}=\left[\begin{array}{c|cccc}\frac{\partial\hat{\mathbf{y}}^e_1}{\partial\mathbf{x}_s} & \frac{\partial\hat{\mathbf{y}}^e_1}{\partial\mathbf{x}_1} & \mathbf{0} & \cdots & \mathbf{0}\\ \frac{\partial\hat{\mathbf{y}}^e_2}{\partial\mathbf{x}_s} & \mathbf{0} & \frac{\partial\hat{\mathbf{y}}^e_2}{\partial\mathbf{x}_2} & \cdots & \mathbf{0}\\ \vdots & \vdots & \vdots & \ddots & \vdots\\ \frac{\partial\hat{\mathbf{y}}^e_{ND}}{\partial\mathbf{x}_s} & \mathbf{0} & \mathbf{0} & \cdots & \frac{\partial\hat{\mathbf{y}}^e_{ND}}{\partial\mathbf{x}_{ND}}\end{array}\right].$$

Again, with bias correction in **Table 1** as an example, the entries in matrices **E** and **F** can be expressed as

$$\begin{aligned}
\frac{\partial \hat{\mathbf{y}}_i^e}{\partial \mathbf{u}_{j\cdot}^e} &= \frac{\partial \mathbf{h}_{yi}}{\partial \mathbf{u}_{j\cdot}^e}\boldsymbol{\beta}_{yi} + \frac{\partial \mathbf{t}_{yi}}{\partial \mathbf{u}_{j\cdot}^e}\mathbf{V}_{\mathbf{d}yi}^{-1}\left(\mathbf{d}_{yi} - \mathbf{H}_{yi}\boldsymbol{\beta}_{yi}\right), \quad i, j = 1,\ldots,ND; i \neq j; \\
\frac{\partial \hat{\mathbf{y}}_i^e}{\partial \mathbf{x}_j} &= \frac{\partial \mathbf{h}_{yi}}{\partial \mathbf{x}_j}\boldsymbol{\beta}_{yi} + \frac{\partial \mathbf{t}_{yi}}{\partial \mathbf{x}_j}\mathbf{V}_{\mathbf{d}yi}^{-1}\left(\mathbf{d}_{yi} - \mathbf{H}_{yi}\boldsymbol{\beta}_{yi}\right), \quad i = 1,\ldots,ND; j = 1,\ldots,ND, s.
\end{aligned} \tag{26}$$

Similar to Eq. (22), it can be proved that $\mathbf{Z}_y$ is uncorrelated with $\mathbf{X}$. Furthermore, assuming $\mathbf{Z}_y$ is uncorrelated with $\mathbf{Z}_u$ (similar to the assumption in Section 3.2 that the elements of $\mathbf{Z}_u$ are uncorrelated), the covariance matrix of the disciplinary outputs is

$$\boldsymbol{\Sigma}_y \approx \left(\mathbf{E}\mathbf{A}^{-1}\mathbf{B} + \mathbf{F}\right)\boldsymbol{\Sigma}_X\left(\mathbf{E}\mathbf{A}^{-1}\mathbf{B} + \mathbf{F}\right)^T + \left(\mathbf{E}\mathbf{A}^{-1}\right)\boldsymbol{\Sigma}_{Zu}\left(\mathbf{E}\mathbf{A}^{-1}\right)^T + \boldsymbol{\Sigma}_{Zy}, \tag{27}$$

where $\boldsymbol{\Sigma}_y$ and $\boldsymbol{\Sigma}_{Zy}$ are the covariance matrices of $\mathbf{y}^e = [\mathbf{y}_1^e; \ldots; \mathbf{y}_{ND}^e]$ and $\mathbf{Z}_y$=[$\mathbf{Z}_{y1}$; …; $\mathbf{Z}_{yND}$], respectively. Similar to the derivation leading up to Eq. (24), $\boldsymbol{\Sigma}_{Zy}$ is approximated by a diagonal matrix

$$\boldsymbol{\Sigma}_{Zy} \approx \operatorname{diag}\left(\sigma_{Zy1}^2(\boldsymbol{\mu}_{x1}, \boldsymbol{\mu}_{xs}, \boldsymbol{\mu}_{u\cdot 1}), \ldots, \sigma_{ZyND}^2(\boldsymbol{\mu}_{xND}, \boldsymbol{\mu}_{xs}, \boldsymbol{\mu}_{u\cdot ND})\right). \tag{28}$$

It can be seen from Eqs. (23) and (27) that the covariance matrices of both the coupling variables and the disciplinary outputs are decomposed into several terms that quantify the impacts of the input variables $\mathbf{X}$ (i.e., $\mathbf{x}_s$ and $\mathbf{x}_{\text{ind}}$) and the model uncertainty $\mathbf{Z}_u$ and $\mathbf{Z}_y$, respectively. $\mathbf{Z}_u$ and $\mathbf{Z}_y$ quantify the uncertainty in the linking variables and responses due to uncertainty in the calibration parameters and in the model discrepancy, as well as the interpolation uncertainty. In the design under uncertainty paradigm, it is important to include them and consider all sources of uncertainty.

In this section, we derived the means and covariance matrices of coupling variables and disciplinary responses considering both aleatory and epistemic uncertainties. The means and covariance of the system QOIs can be derived similarly, in a straightforward

manner. When the system QOI is an analytical function of subsystem responses, e.g. the sum of weights of disciplinary components in a vehicle design, propagating the uncertainty from disciplinary responses to system QOIs is trivial. When system level analyses also involve aleatory uncertainty and/or epistemic uncertainty, it can be treated as a single-disciplinary UP problem, and can be solved using any existing UP method as an add-on to the MUA method.

4 CASE STUDY: ELECTRONIC PACKAGING

To demonstrate the effectiveness of the proposed SRP-based MUA method, in this section we consider a design problem in electronic packaging [51], which is a benchmark multidisciplinary problem that has been frequently studied in the literature [28, 30, 52-54]. In this test problem, a circuit consisting of two resistors is mounted on a heat sink. It comprises the coupling between electrical and thermal subsystems, as demonstrated in **Figure 4**. There are eight input variables x_1—x_8, five linking variables y_6, y_7, y_{11}, y_{12}, y_{13}, and three system QOIs y_1, y_4, and y_5. The numbering is to be consistent with the aforementioned works that considered this problem. Variables not indicated in the figure, such as y_2 and y_3, are intermediate variables that are not of interest in this analysis. Following the notation in Section 3, we denote $\mathbf{x}_1=\{x_5, x_6, x_7, x_8\}^T$, $\mathbf{x}_2=\{x_1, x_2, x_3, x_4\}^T$, $\mathbf{u}_{12}=\{y_6, y_7\}^T$, $\mathbf{u}_{21}=\{y_{11}, y_{12}, y_{13}\}^T$, and $\mathbf{y}_1=\{y_1, y_4, y_5\}^T$. **Table 2** provides the physical meanings of the input/output variables of interest; a detailed problem statement that includes descriptions of all variables can be found in the referenced literature. The two disciplines are coupled so that the two component resistances needed in the electrical discipline depend on operating temperatures, which are output from the thermal discipline,

while the operating temperatures in the thermal discipline depend on the resistances from the electrical discipline.

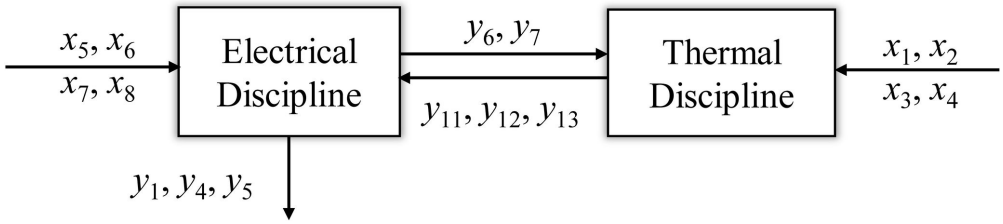

Figure 4. Electronic packaging problem

Table 2. Design variables and state variables in the electronic packaging problem

x_1	Heat sink width (m)	y_1	Negative of watt density ($watts/m^3$)
x_2	Heat sink length (m)	y_4	Current in resistor #1 ($amps$)
x_3	Fin length (m)	y_5	Current in resistor #2 ($amps$)
x_4	Fin width (m)	y_6	Power dissipation in resistor #1 ($watts$)
x_5	Nominal resistance #1 at temperature $20°C$ (Ω)	y_7	Power dissipation in resistor #2 ($watts$)
x_6	Temperature coefficient of electrical resistance #1 ($°K^{-1}$)	y_{11}	Component temperature of resistor #1 ($°C$)
x_7	Nominal resistance #2 at temperature $20°C$ (Ω)	y_{12}	Component temperature of resistor #2 ($°C$)
x_8	Temperature coefficient of electrical resistance #2 ($°K^{-1}$)	y_{13}	Heat sink volume (m^3)

The original design objective is to maximize the watt density for the package subject to several constraints, i.e.

$$\begin{aligned} &\min \quad y_1 \\ &s.t. \quad y_4 - y_5 \le 0, \quad y_{11} \le 85, \quad y_{12} \le 85. \end{aligned} \tag{29}$$

To test our proposed approach, we modified the original problem as follows. Since the thermal discipline is much more complex than the electrical discipline, and it requires a finite difference strategy to calculate the component temperatures, we assume that the models to evaluate y_{11}, y_{12}, given $\{x_1, x_2, x_3, x_4, y_6, y_7\}$ in the thermal discipline may be inaccurate and require model uncertainty quantification. We first collected data from

simulations and experiments and conducted disciplinary model bias correction (Section 4.1), and then used the updated SRP emulators for system analysis (Section 4.2). We then assessed the uncertainty stemming from input variability and model uncertainty (of y_{11} and y_{12}) as it propagates to the system QOIs, and we compared the results with conventional MCS. Finally, we applied the proposed approach for achieving a robust design solution and examine the impact of epistemic uncertainty (Section 4.3).

4.1 Disciplinary Model Uncertainty Quantification

We first collected data comprised of 40 "experimental" observations. Since the original benchmark problem does not consider epistemic uncertainty, nor does it contain experimental data, we generated a set of hypothetical experimental testing data for y_{11} and y_{12} by adding zero-mean random noises to the exact model provided in [51]. The 40 experimental runs were determined via a Latin Hypercube space filling design over the six-dimensional input space for $\{x_1, x_2, x_3, x_4, y_6, y_7\}$. We then collected additional data comprised of 60 simulation observations of y_{11} and y_{12} from a low-fidelity simulation model that we built by intentionally adding a nonlinear model bias function $\boldsymbol{\delta}(\mathbf{x})$ to the exact model. This bias function was chosen to result in a significant discrepancy between the simulation data and the exact model. The 60 simulation runs were also determined via a (different) Latin Hypercube design, so that the $\mathbf{x}$ locations are completely different than those for the experimental runs. Integrating the two sets of data, we applied the SRP-based bias correction approach discussed in Section 2.1 to quantify the model uncertainty and to subsequently obtain an updated emulator for both y_{11} and y_{12}. To ensure that the emulator we obtain is valid for analysis and design, a validation step was performed for 20 random input settings. The emulator (after incorporating a correction for the estimated bias via the

equations in **Table 1**) was compared to the actual response (from [51]) in **Figure 5** for y_{11}, for illustration purposes.

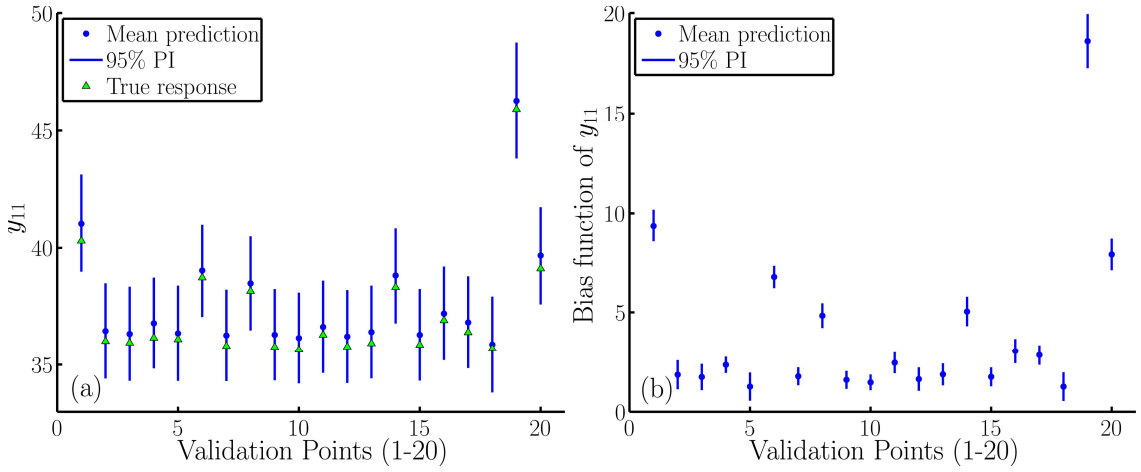

Figure 5. (a) Model prediction (after model bias correction) and (b) estimation of bias function for linking variable y_{11}

In **Figure 5**, both the model predictions and the estimation of bias function are shown, and a 95% prediction interval (PI) is plotted for all 20 predictions. It can be seen that the rather large model bias was effectively captured by the uncertainty quantification process, and the predictions after incorporating the bias correction are all quite close to the actual responses. Also, the 95% PIs cover the actual responses and provide a reasonable assessment of model predictive uncertainty.

4.2 Evaluation of Mean and (Co)Variance of System QOIs

Here we conduct the UP analysis considering the impact of both input variability (aleatory) and model uncertainty (epistemic) on the system QOIs. Given the following information that $x_1 \sim \mathcal{N}(0.1, 0.01^2)$, $x_2 \sim \mathcal{N}(0.1, 0.01^2)$, $x_3 \sim \mathcal{N}(0.1, 0.01^2)$, $x_4 \sim \mathcal{N}(0.02, 0.01^2)$, $x_5 \sim \mathcal{N}(500, 10^2)$, $x_6 \sim \mathcal{N}(0.005, 0.001^2)$, $x_7 \sim \mathcal{N}(500, 10^2)$, $x_8 \sim \mathcal{N}(0.005, 0.001^2)$, we apply the proposed SRP-based MUA method to find the means and standard deviations (STDs) of

y_1, y_4, y_5, y_6, y_7, y_{11}, y_{12}, y_{13}. First, we replace the simulation models of y_{11} and y_{12} by their updated SRP emulators, and obtain the means of the y variables from Eqs. (16)~(17). We then analytically construct the **A**, **B**, **E**, **F** matrices, and finally evaluate the STDs of the y variables using these matrices as we present in Eqs. (23) and (27). For the purpose of validating our method, we also used a conventional MCS to evaluate the same quantities. MCS considering aleatory uncertainty is straightforward; however complexity arises when epistemic uncertainty is also included. We adopted a nested two-level MCS: in the outer loop, random samples are generated for input variables; in the inner loop, another sampling is applied to find the distributions of linking variables, under a fixed input setting. The whole process is very computationally challenging.

A comparison between the results of MUA and MCS is shown in **Table 3**. We also list the standard deviations of the outputs considering only model uncertainty (i.e., by setting the input standard deviations to zero), to demonstrate the impact of epistemic uncertainty. The MUA method provides good agreement with the MCS. Regarding computational costs, MCS takes around six hours on a high-end computer, while our MUA method takes only 1~2 seconds, which is a huge saving. **Figure 6** illustrates the probability distributions of selected responses y_1, y_4 via their histograms from the MCS. The distributions are neither highly skewed nor highly kurtic, which implies that for this example evaluating first two moments is sufficient for robust design and reliability-based design.

Table 3. Evaluation of means and variances of responses

	Mean		STD		STD with only model uncertainty	
	MCS	MUA	MCS	MUA	MCS	MUA
y_1	−380.6889	−368.9532	68.886550	64.306658	1.195891	1.184757
y_4	0.018458	0.018445	0.000475	0.000477	0.000086	0.000085
y_5	0.018462	0.018450	0.000475	0.000477	0.000083	0.000082
y_6	0.184577	0.184454	0.004754	0.004726	0.000856	0.000851
y_7	0.184619	0.184499	0.004753	0.004716	0.000834	0.000823
y_{11}	36.847740	36.856404	1.017308	1.003813	1.006827	1.000991

y_{12}	36.807522	36.802927	0.990697	0.970557	0.980447	0.967040
y_{13}	0.001000	0.001000	0.000174	0.000173	0	0

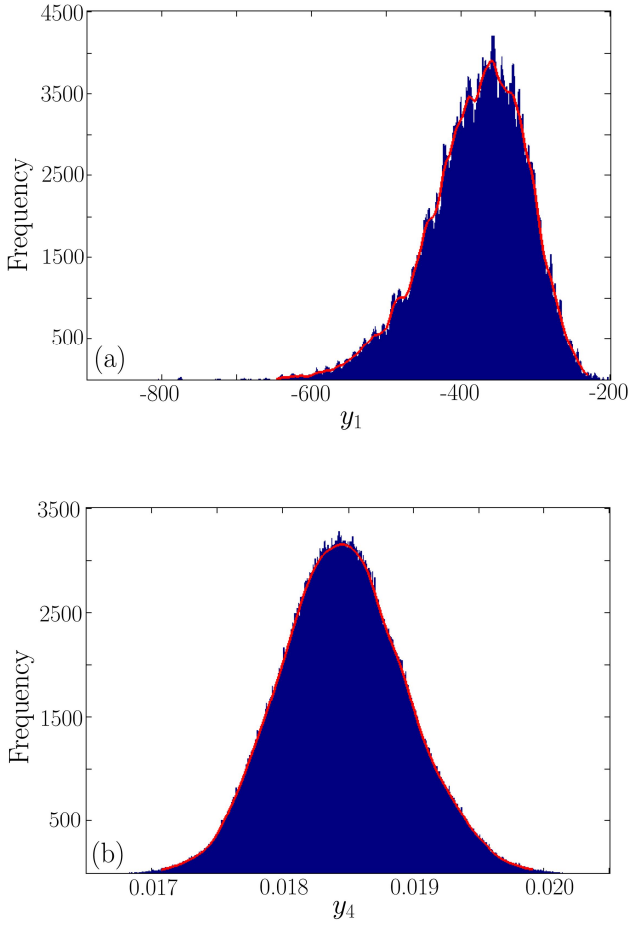

Figure 6. Histograms of system QOIs: (a) y_1 and (b) y_4

In this example, it appears that many of the responses are not correlated. We select a few response pairs and calculated their correlation coefficients via both MCS and the MUA method (from Eq. (26)), the results of which are shown in **Table 4**. Again the proposed MUA method is in fairly good accordance with MCS. Another interesting observation is that the existence of epistemic uncertainty dramatically alters the correlation between responses, changing some of them (e.g. y_6 and y_{11}) from positively correlated to negatively correlated for this example. **Figure 7** further illustrates this with scatter plots of the

response pairs over the Monte Carlo samples. In general, the presence of epistemic uncertainty may either amplify or mitigate the correlation between responses, depending on the specifics of the problem. If the change in the correlation is drastic, it means that the impact of epistemic uncertainty is notable and the model should be carefully examined.

Table 4. Correlation coefficient between selected responses

	Considering both uncertainties		Considering aleatory uncertainty only	
	MCS	MUA	MCS	MUA
y_6 and y_{11}	−0.1818	−0.1532	0.3522	0.3591
y_7 and y_{12}	−0.2039	−0.1447	0.3538	0.3482
y_{11} and y_{13}	~0	~0	0.6353	0.5849
y_{12} and y_{13}	~0	~0	0.2224	0.2384

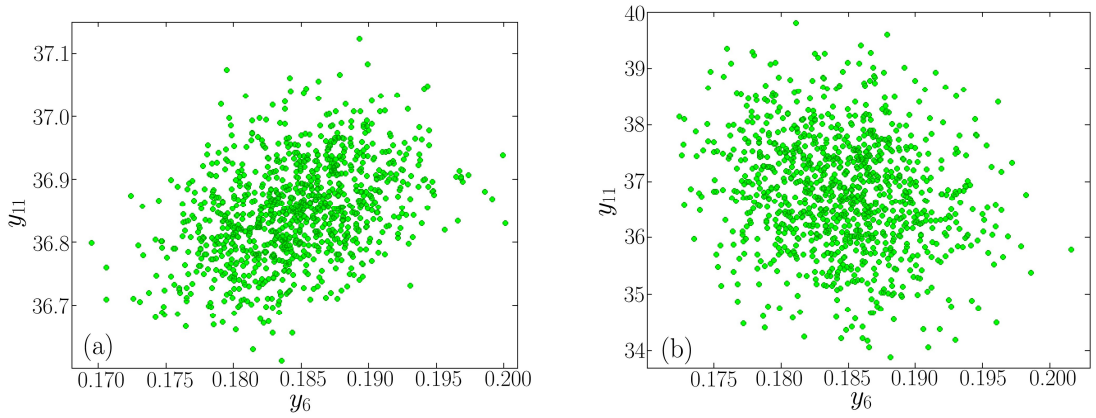

Figure 7. Scatter plots of y_6 and y_{11} (a) considering only aleatory uncertainty (for which they are positively correlated), and (b) considering both uncertainties (for which they are negatively correlated)

4.3 Examination of Impact of Epistemic Uncertainty on Design Optimization

Having the uncertainties considered, the original deterministic design optimization problem (Eq. (29)) is reformulated as a robust design version (as seen in [30]), i.e.

$$\begin{aligned} \min \quad & \mu_{y_1} + k_0\sigma_{y_1} \\ s.t. \quad & \mu_{(y_4-y_5)} + k_1\sigma_{(y_4-y_5)} \le 0, \\ & \mu_{y_{11}} + k_2\sigma_{y_{11}} \le 85, \quad \mu_{y_{12}} + k_3\sigma_{y_{12}} \le 85, \end{aligned} \tag{30}$$

which aims at achieving a larger expected watt density ($-\mu_{y_1}$) that is at the same time less sensitive to the variation in design variables and epistemic model uncertainty. k_i (i=0,1,2,3) are a set of user-selected coefficients that balance the relative importance of minimizing the mean versus variation about the mean; a large value of k_0, for example, indicates that a less variant system performance is desired while a lower mean watt density is tolerated. In this subsection we solve the design optimization problem under three different scenarios: 1) deterministic optimization without considering any uncertainty (Eq. (29)); 2) robust design optimization considering aleatory uncertainty only; and 3) robust design optimization considering both aleatory and epistemic uncertainties. The optimum solutions are listed in **Table 5**.

Table 5. Optimum solutions of the electronic packaging problem

Scenario	x_1	x_2	x_3	x_4	x_5	x_6	x_7	x_8	μ_{y1}
1	0.0500	0.0500	0.0100	0.0500	10.00	0.0040	10.00	0.0040	-6.9655×10^5
2	0.0500	0.0500	0.0108	0.0050	658.61	0.0090	10.00	0.0040	-3.1344×10^5
3	0.0500	0.0500	0.0101	0.0053	388.12	0.0040	292.60	0.0040	-2.2229×10^4

It is clear that considering uncertainty compromises the system performance (y_1 in this case). The expected value of y_1 is increasing, corresponding to a decrease of watt density of the electronic package, as we try to achieve a design solution that is robust to more sources of uncertainty. **Figure 8** further depicts how uncertainty influences the design solution by plotting the variances of y_1 (used in the objective function), y_{11} and y_{12} (linking variables used in the constraints) contributed by aleatory uncertainty and epistemic uncertainty, respectively. It is clear that the solution from scenario 1 using a deterministic optimization formulation is significantly affected by uncertainty (mostly aleatory) and therefore is not robust. The solution from scenario 2 considering aleatory uncertainty only

yields much better robustness, however the impact of model uncertainty may outweigh the impact of input variability (as seen in scenario 2 in **Figure 8(c)**), which would violate the third constraint on y_{12} in formulation (30) if model uncertainty is included. Finally, the solution from scenario 3 that considers both aleatory and epistemic uncertainties in the design formulation has the best mitigation over all sources of uncertainty, while the mean system performance is somewhat sacrificed.

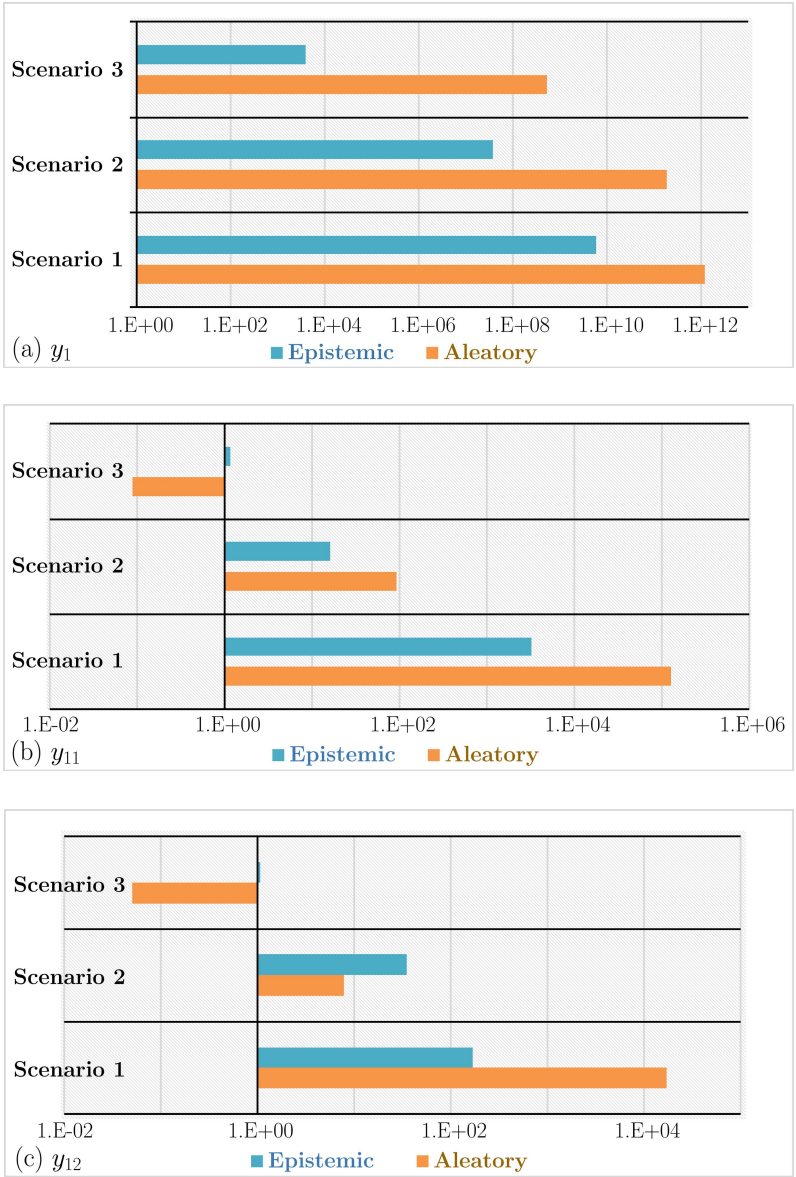

Figure 8. Variances of (a) y_1, (b) y_{11} and (c) y_{12} contributed by aleatory and epistemic uncertainties in three different scenarios

Although it has a significant impact on the correlation of responses and the final design solution in **Table 5**, it appears from **Table 3** and **Figure 8** that, for this example, model uncertainty generally has less impact on the variances of y_1—y_7, compared to the impact of input variability. This is because we have gathered a sufficient amount of data (40 "experiments" and 60 simulations for six-dimensional models of y_{11} and y_{12}) in this example for model updating, and hence the uncertainty in the calibrated and bias-corrected model is very small, as is shown in **Figure 5(a)**. Specifically, at the mean value of the design setting described in Section 4.2, the root MSE of the y_{11} and y_{12} predictions (which can be interpreted as the disciplinary model prediction STD) is found to be $\boldsymbol{\sigma}_{Zu} \equiv (\text{diag}(\boldsymbol{\Sigma}_{Zu}))^{1/2} = (0.5031, 0.4862)$, which is roughly only 1% of the mean predictions of y_{11} and y_{12}. On the other hand, the standard deviations of input variables are roughly 10% of their nominal values. For this example, the impact of input variability dominates. However, we do expect a much larger impact of model uncertainty if the model uncertainty is larger. **Figure 9** and **Figure 10** plot the multiplicative increase in QOI STD and the proportion of system QOI total variance that results from model uncertainty, respectively, versus a multiplicative increase in the model prediction STD $\boldsymbol{\sigma}_{Zu}$. For example, if $\boldsymbol{\sigma}_{Zu}$ is increased by a factor of 10 (in which case it is around 10% of the mean prediction and on par with aleatory uncertainty), then the STDs of both y_4 and y_5 would be more than twice as large as currently in **Table 3**, and the impact of model uncertainty accounts for 80% of the total variance of y_4 and y_5. As a result, we believe that in general engineering applications, model uncertainty is a factor that should not be neglected. The epistemic uncertainty in the original example was fairly small, only because we already collected a

sufficiently large data set and corrected the emulators to a satisfactory level.

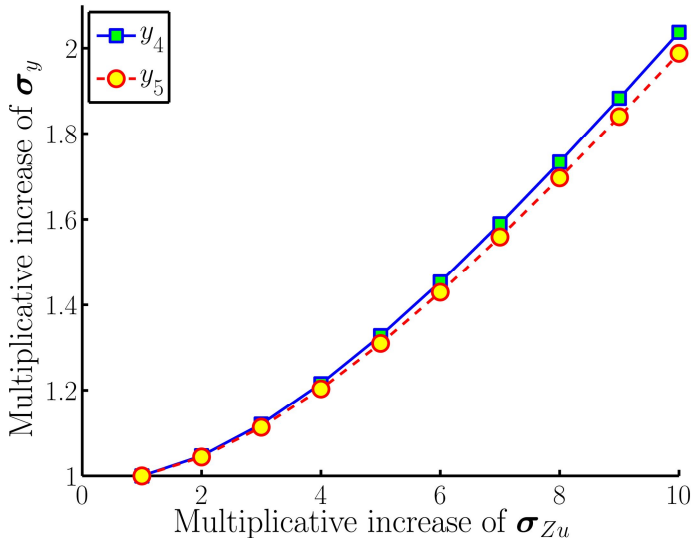

Figure 9. Relationship between a multiplicative increase in model uncertainty and the resulting increase in the system QOIs' STD

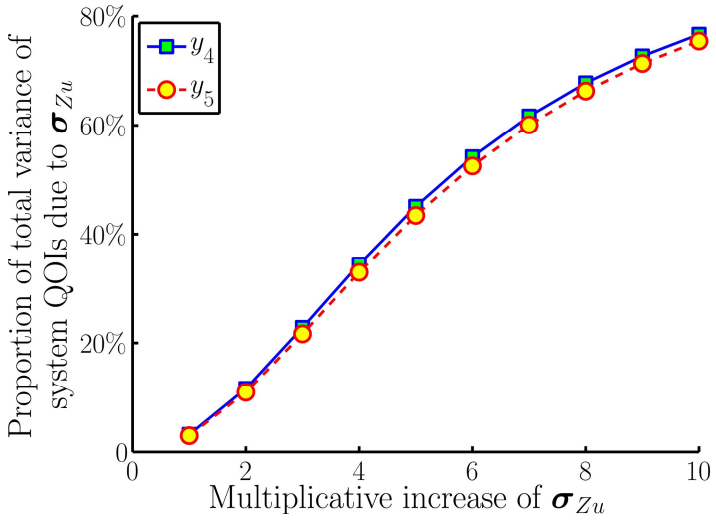

Figure 10. Relationship between a multiplicative increase in model uncertainty and the resulting increase in the proportion of total variance of system QOIs due to model uncertainty

Analyzing the impact of model uncertainty has many potential usages, one of which is for resource allocation to reduce the system level uncertainty by collecting additional simulation and/or experimental data for selected disciplines. For example, in the original

electronic packaging problem, y_{11} and y_{12} are used for system optimization constraints. Model uncertainty that is too high may lead to an overly conservative design solution. If the designer is not comfortable with the current amount of model uncertainty, additional data can be collected over the regions where y_{11} and y_{12} are most influenced by model uncertainty. **Figure 11** illustrates the impact of model uncertainty by plotting the prediction error variances (due to epistemic uncertainty) of y_{11} and y_{12} as x_1 and x_2 varies over the design region. Regions with higher variance are where more data should be collected.

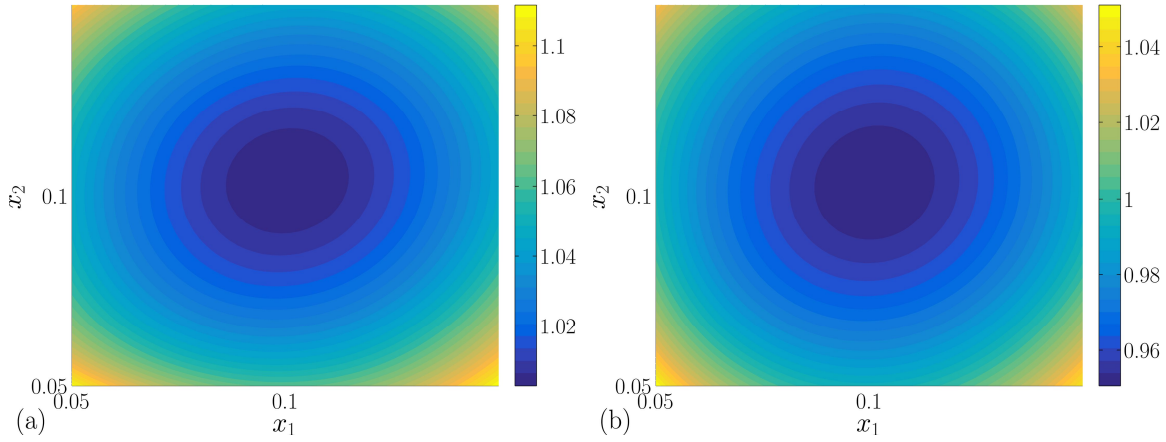

Figure 11. Contour plots of the variances of (a) y_{11} and (b) y_{12} induced by model uncertainty over the design region of x_1 and x_2

5 CONCLUSIONS

Uncertainty propagation is critically important in multidisciplinary design optimization. Most prior work does not consider epistemic uncertainty, especially model uncertainty, although we have demonstrated that this can have a significant impact on the system level uncertainty. Our approach accounts for disciplinary model uncertainty through decomposition of coupled disciplines, resulting in a fast but accurate assessment, and an efficient SRP-based MUA method was developed to propagate multiple sources of uncertainties from disciplinary inputs and models to the system quantities of interests. Our

approach first applies SRP-based modeling to quantify disciplinary model uncertainties and obtain disciplinary SRP emulators, and then estimates the lower-order statistical moments of system QOIs based on a Taylor series expansion. The tractable structure of SRP emulators is fully utilized so that the approach leads to compact analytical formulas. Compared with traditional uncertainty propagation methods in MDO that consider both aleatory and epistemic uncertainty, our approach yields a significant saving in computational cost; it enables uncertainty propagation for strongly coupled MDO systems while most other methods like MCS are unlikely to be feasible. The computational complexity of the method only resides in the inversion of matrix **A** [which is a matrix relating the linking variables, as appears in Eq. (27)], and hence it can handle a system with a reasonable number of linking variables as long as the matrix inversion of **A** is feasible.

Furthermore, the proposed method is applicable to both feed-forward and feedback coupling relationships between different disciplines. We consider it extremely useful in the situation when only the mean and (co)variance of system QOIs are of interest (e.g. in a robust design scenario), in which case the method is independent of the particular form of distribution for the input variables. A benchmark electronic packaging problem was used to show that the proposed MUA method is effective and extremely efficient in evaluating the means and variances of system QOIs.

The limitation of the proposed work is that the 1st-order Taylor expansion would not be accurate if the model is highly nonlinear over the range of input variation. We plan to improve the proposed method in this aspect as future work. We also plan to incorporate our proposed method as a part of multidisciplinary design optimization framework, including performing multidisciplinary statistical sensitivity analysis to evaluate the

relative contributions of aleatory and epistemic uncertainties, developing a rigorous resource allocation scheme to reduce the system level uncertainty, etc. We anticipate that the proposed SRP-based MUA method will significantly accelerate many analyses in multidisciplinary design while maintain good accuracy.

ACKNOWLEDGMENT

The grant support from the National Science Foundation (CMMI-1233403) is greatly acknowledged. Wei Li's predoctoral visit at Northwestern University is sponsored by the China Scholarship Council.

NOMENCLATURE

$\mathbf{x}=(x_1, \ldots, x_p)$	p-dimensional input variable
$\boldsymbol{\theta}=(\theta_1, \ldots, \theta_r)$	r-dimensional unknown model parameter
$\boldsymbol{\theta}^*$	true values of unknown model parameter
$f(\cdot)$	a Gaussian process (GP)
$m(\cdot)$	mean function of GP
$V(\cdot,\cdot)$	covariance function of GP
$\boldsymbol{\phi}$	hyperparameters of GP
$y^m(\cdot)$, $y^e(\cdot)$	simulation/experimental response
$\delta(\cdot)$	model bias function
ε	experimental error
$\mathbf{X}^m$, $\mathbf{X}^e$	input settings when conducting simulations/experiments
$\boldsymbol{\Theta}^m$	settings of model parameters when conducting simulations
$\mathbf{d}$	collected data
$\mathbf{h}^m(\cdot)$, $\mathbf{h}^\delta(\cdot)$	prespecified basis function for polynomial regression of mean function of simulation model GP / bias function GP
$\boldsymbol{\beta}^m$, $\boldsymbol{\beta}^\delta$	coefficients for polynomial regression of mean function of simulation model GP / bias function GP
$V^m(\cdot,\cdot)$, $V^\delta(\cdot,\cdot)$	covariance function of simulation model GP / bias function GP
$p(\boldsymbol{\phi} \mid \mathbf{d})$	likelihood function in SRP modeling and model bias correction
$p(\boldsymbol{\phi} \mid \mathbf{d}, \boldsymbol{\theta})$	likelihood function in Bayesian model calibration
$p(\boldsymbol{\theta})$	prior distribution of unknown model parameter $\boldsymbol{\theta}$
$p(\boldsymbol{\theta} \mid \mathbf{d}, \boldsymbol{\phi})$	posterior distribution of unknown model parameter $\boldsymbol{\theta}$
$\hat{y}^e(\cdot)$	mean prediction of the experimental response from the updated model
$\mathrm{MSE}\left(\hat{y}^e(\cdot)\right)$	mean squared error of the mean prediction of the experimental response
$Z(\cdot)$	a random quantity representing model uncertainty in prediction
$\sigma_Z^2(\cdot)$	variance of $Z(\cdot)$; mathematically equal to $\mathrm{MSE}\left(\hat{y}^e(\cdot)\right)$
ND	number of disciplines
$\mathbf{x}_i$, $\mathbf{x}_{\text{ind}}$	disciplinary input variables of the ith discipline / all ND disciplines
$\mathbf{x}_s$	shared input variables across disciplines
$\mathbf{X}$	a complete set of input variables, including both $\mathbf{x}_{\text{ind}}$ and $\mathbf{x}_s$
$\mathbf{u}_{ij}$	linking variables; output from the ith discipline and input to the jth discipline
$\mathbf{y}_i$, $\mathbf{y}_{\text{ind}}$	disciplinary outputs of the ith discipline / all ND disciplines
$\mathbf{y}_{\text{sys}}$	system quantities of interest (QOIs)
$\boldsymbol{\mu}$	a mean vector; subscript, if available, denotes a specific random quantify, e.g. $\boldsymbol{\mu}_{xs}$ refers to the mean of shared input variables $\mathbf{x}_s$
$\boldsymbol{\Sigma}$	a covariance matrix; subscript, if available, denotes a specific random quantify, e.g. $\boldsymbol{\Sigma}_{xs}$ refers to the covariance of shared input variables $\mathbf{x}_s$

REFERENCES

[1] Shubin, G.R., *Optimization Problem Formulation for Multidisciplinary Design.* Inverse Problems and Optimal Design in Industry, Proceedings of the Conference, 1994. **10**: p. 213-216.

[2] Alexandrov, N.M. and R.M. Lewis, *Algorithmic Perspectives on Problem Formulations in MDO.* AIAA Paper, 2000. **4719**: p. 2000.

[3] Belytschko, T., *Fluid-Structure Interaction.* Computers & Structures, 1980. **12**(4): p. 459-469.

[4] McNamara, J.J. and P.P. Friedmann, *Aeroelastic and Aerothermoelastic Analysis in Hypersonic Flow: Past, Present, and Future.* AIAA Journal, 2011. **49**(6): p. 1089-1122.

[5] Yao, W., X.Q. Chen, W.C. Luo, M. van Tooren, and J. Guo, *Review of Uncertainty-Based Multidisciplinary Design Optimization Methods for Aerospace Vehicles.* Progress in Aerospace Sciences, 2011. **47**(6): p. 450-479.

[6] Matthies, H.G., *Quantifying Uncertainty: Modern Computational Representation of Probability and Applications.* Extreme Man-Made and Natural Hazards in Dynamics of Structures, 2007: p. 105-135.

[7] Kiureghian, A.D. and O. Ditlevsen, *Aleatory or Epistemic? Does It Matter?* Structural Safety, 2009. **31**(2): p. 105-112.

[8] Kennedy, M.C. and A. O'Hagan, *Bayesian Calibration of Computer Models.* Journal of the Royal Statistical Society Series B-Statistical Methodology, 2001. **63**: p. 425-450.

[9] Zaman, K. and S. Mahadevan, *Robustness-Based Design Optimization of Multidisciplinary System Under Epistemic Uncertainty.* Aiaa Journal, 2013. **51**(5): p. 1021-1031.

[10] Helton, J.C., J.D. Johnson, C.J. Sallaberry, and C.B. Storlie, *Survey of sampling-based methods for uncertainty and sensitivity analysis.* Reliability Engineering & System Safety, 2006. **91**(10-11): p. 1175-1209.

[11] Landau, D.P. and K. Binder, *A guide to Monte Carlo simulations in statistical physics*. 2 ed. 2005, New York: Cambridge University Press.

[12] Robert, C. and G. Casella, *Monte Carlo Statistical Methods*. 1999, New York: Springer.

[13] Thoft-Cristensen, P. and M.J. Baker, *Structural Reliability Theory and Its Applications*. 1982, New York: Springer.

[14] Green, L.L., H.-Z. Lin, and M.R. Khalessi, *Probabilistic methods for uncertainty propagation applied to aircraft design.* AIAA Paper, 2002. **3140**: p. 2002.

[15] Cao, H. and B. Duan, *Uncertainty Analysis for Multidisciplinary Systems Based on Convex Models*, in *10th AIAA/ISSMO Multidisciplinary Analysis and Optimization Conference*. 2004: Albany, New York.

[16] Du, X., J. Guo, and H. Beeram, *Sequential optimization and reliability assessment for multidisciplinary systems design.* Structural and Multidisciplinary Optimization, 2008. **35**(2): p. 117-130.

[17] Guo, J. and X.P. Du, *Reliability Analysis for Multidisciplinary Systems with Random and Interval Variables.* Aiaa Journal, 2010. **48**(1): p. 82-91.

[18] Gu, X. and J.E. Renaud. *Implementation study of implicit uncertainty propagation (IUP) in decomposition-based optimization*. in *Proceedings of the 9th*

AIAA/USAF/NASA/ISSMO Symposium on Multidisciplinary Analysis and Optimization, AIAA-2002-5416, Atlanta, Georgia. 2002.

[19] Gu, X.S., J.E. Renaud, and C.L. Penninger, *Implicit uncertainty propagation for robust collaborative optimization.* Journal of Mechanical Design, 2006. **128**: p. 1001.

[20] Du, X. and W. Chen. *Collaborative reliability analysis for multidisciplinary systems design*. in *Proceedings of the 9th AIAA/USAF/NASA/ISSMO Symposium on Multidisciplinary Analysis and Optimization*. 2002.

[21] Du, X. and W. Chen, *Collaborative reliability analysis under the framework of multidisciplinary systems design.* Optimization and Engineering, 2005. **6**(1): p. 63-84.

[22] Xiong, F., X. Yin, W. Chen, and S. Yang, *Enhanced probabilistic analytical target cascading with application to multi-scale design.* Engineering Optimization, 2010. **42**(6): p. 581-592.

[23] Sankararaman, S. and S. Mahadevan, *Likelihood-Based Approach to Multidisciplinary Analysis Under Uncertainty.* Journal of Mechanical Design, 2012. **134**(3).

[24] Liang, C. and S. Mahadevan, *Stochastic Multidisciplinary Analysis with High Dimensional Coupling*, in *10th World Congress on Structural and Multidisciplinary Optimization*. 2013: Orlando, Florida, USA.

[25] Sankararaman, S. and S. Mahadevan, *Likelihood-based representation of epistemic uncertainty due to sparse point data and/or interval data.* Reliability Engineering & System Safety, 2011. **96**(7): p. 814-824.

[26] Zhang, S.L., P. Zhu, W. Chen, and P. Arendt, *Concurrent treatment of parametric uncertainty and metamodeling uncertainty in robust design.* Structural and Multidisciplinary Optimization, 2013. **47**(1): p. 63-76.

[27] Gu, X., J.E. Renaud, S.M. Batill, R.M. Brach, and A.S. Budhiraja, *Worst case propagated uncertainty of multidisciplinary systems in robust design optimization.* Structural and Multidisciplinary Optimization, 2000. **20**(3): p. 190-213.

[28] Du, X. and W. Chen. *An efficient approach to probabilistic uncertainty analysis in simulation-based multidisciplinary design*. in *38th AIAA Aerospace Sciences Meeting and Exhibit*. 2000. Reno, NV.

[29] Du, X. and W. Chen, *Methodology for managing the effect of uncertainty in simulation-based design.* AIAA Journal, 2000. **38**(8): p. 1471-1478.

[30] Du, X. and W. Chen, *Efficient uncertainty analysis methods for multidisciplinary robust design.* AIAA Journal, 2002. **40**(3): p. 545-552.

[31] Jiang, X.M. and S. Mahadevan, *Bayesian hierarchical uncertainty quantification by structural equation modeling.* International Journal for Numerical Methods in Engineering, 2009. **80**(6-7): p. 717-737.

[32] Jiang, X.M. and S. Mahadevan, *Bayesian structural equation modeling method for hierarchical model validation.* Reliability Engineering & System Safety, 2009. **94**(4): p. 796-809.

[33] Sankararaman, S., K. McLemore, S. Mahadevan, S.C. Bradford, and L.D. Peterson, *Test Resource Allocation in Hierarchical Systems Using Bayesian Networks.* AIAA Journal, 2013. **51**(3): p. 537-550.

[34] Allaire, D., Q. He, J. Deyst, and K. Willcox, *An Information-Theoretic Metric of System Complexity with Application to Engineering System Design.* Journal of Mechanical Design, 2012. **134**(10): p. 100906.

[35] Sacks, J., W.J. Welch, T.J. Mitchell, and H.P. Wynn, *Design and analysis of computer experiments.* Statistical Science, 1989. **4**(4): p. 409-423.
[36] Conti, S., J.P. Gosling, J.E. Oakley, and A. O'Hagan, *Gaussian process emulation of dynamic computer codes.* Biometrika, 2009. **96**(3): p. 663-676.
[37] Conti, S. and A. O'Hagan, *Bayesian emulation of complex multi-output and dynamic computer models.* Journal of Statistical Planning and Inference, 2010. **140**(3): p. 640-651.
[38] Higdon, D., M. Kennedy, J.C. Cavendish, J.A. Cafeo, and R.D. Ryne, *Combining field data and computer simulations for calibration and prediction.* Siam Journal on Scientific Computing, 2004. **26**(2): p. 448-466.
[39] Higdon, D., J. Gattiker, B. Williams, and M. Rightley, *Computer model calibration using high-dimensional output.* Journal of the American Statistical Association, 2008. **103**(482): p. 570-583.
[40] Arendt, P.D., D.W. Apley, and W. Chen, *Quantification of Model Uncertainty: Calibration, Model Discrepancy, and Identifiability.* Journal of Mechanical Design, 2012. **134**(10).
[41] Arendt, P.D., D.W. Apley, W. Chen, D. Lamb, and D. Gorsich, *Improving Identifiability in Model Calibration Using Multiple Responses.* Journal of Mechanical Design, 2012. **134**(10).
[42] Jiang, Z., W. Chen, Y. Fu, and R.-J. Yang, *Reliability-Based Design Optimization with Model Bias and Data Uncertainty.* SAE International Journal of Materials & Manufacturing, 2013. **6**(3): p. 502-516.
[43] Rasmussen, C.E. and C.K.I. Williams, *Gaussian Processes for Machine Learning*. 2006: The MIT Press.
[44] Kennedy, M.C. and A. O'Hagan, *Predicting the output from a complex computer code when fast approximations are available.* Biometrika, 2000. **87**(1): p. 1-13.
[45] Hasselman, T.K., K. Yap, C.-H. Lin, and J.A. Cafeo, *A case study in model improvement for vehicle crashworthiness simulation*, in *23rd International Modal Analysis Conference*. 2005: Orlando, FL.
[46] Chen, W., Y. Xiong, K.L. Tsui, and S. Wang, *A design-driven validation approach using Bayesian prediction models.* Journal of Mechanical Design, 2008. **130**(2).
[47] Qian, P.Z.G. and C.F.J. Wu, *Bayesian hierarchical modeling for integrating low-accuracy and high-accuracy experiments.* Technometrics, 2008. **50**(2): p. 192-204.
[48] Wang, S.C., W. Chen, and K.L. Tsui, *Bayesian Validation of Computer Models.* Technometrics, 2009. **51**(4): p. 439-451.
[49] Bayarri, M.J., J.O. Berger, R. Paulo, J. Sacks, J.A. Cafeo, J. Cavendish, C.H. Lin, and J. Tu, *A framework for validation of computer models.* Technometrics, 2007. **49**(2): p. 138-154.
[50] Liu, F., M.J. Bayarri, J.O. Berger, R. Paulo, and J. Sacks, *A Bayesian analysis of the thermal challenge problem.* Computer Methods in Applied Mechanics and Engineering, 2008. **197**(29-32): p. 2457-2466.
[51] Salas, A.O. *MDO Test Suite*. 1995; Available from: http://www.eng.buffalo.edu/Research/MODEL/mdo.test.orig/class2prob3.html.
[52] Renaud, J. and G. Gabriele, *Approximation in nonhierarchic system optimization.* AIAA journal, 1994. **32**(1): p. 198-205.
[53] Padula, S.L., N. Alexandrov, and L.L. Green, *MDO test suite at NASA Langley*

Research Center. AIAA Paper, 1996(96-4028).
[54] Kodiyalam, S. and J. Sobieszczanski-Sobieski, *Multidisciplinary design optimization - some formal methods, framework requirements, and application to vehicle design.* International Journal of Vehicle Design, 2001. **25**(1-2): p. 3-22.

List of Tables

List of Figures